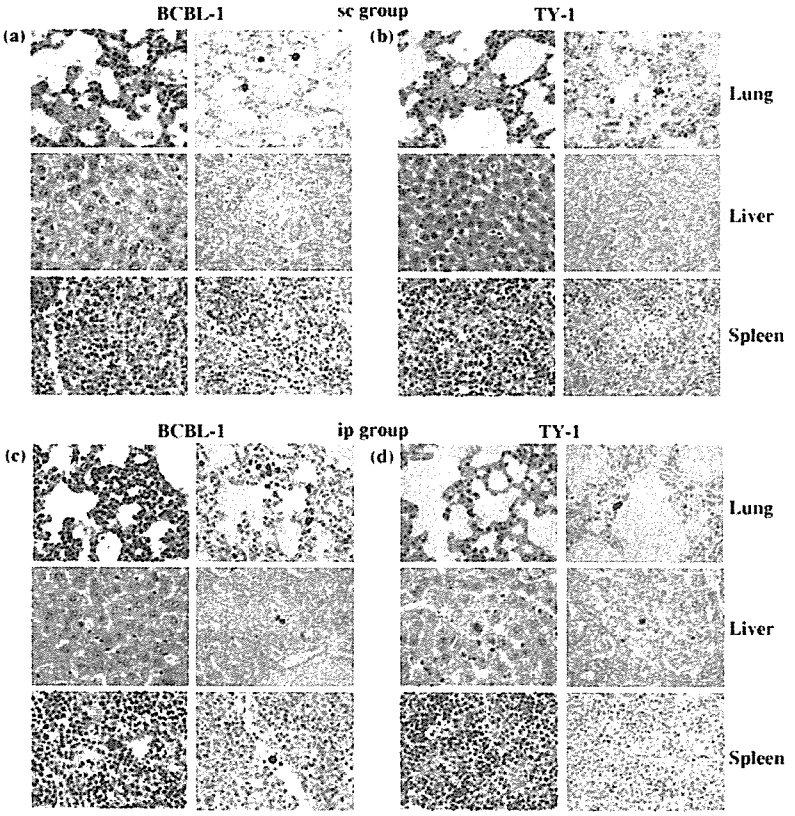

Fig. 2. Metastasis of primary effusion lymphoma (PEL) cells in various organs of T, B and natural killer (NK) knock-out NOG mice. (a–d) Histological analysis of lung, liver and spleen of mice inoculated with BCBL-1 and TY-1 cells either (a,b) subcutaneously (sc) or (c,d) intraperitonealy (ip). Immunohistochemical staining was conducted using anti-LANA. Data are from (a,c) BCBL-1-inoculated mice and (b,d) TY-1-inoculated mice. Left and right panels of all figures represent hematoxylin–eosin and immunostaining, respectively (magnification, ×40).

NOG mice have a defective common cytokine receptor, γ chain. Mutation in the common cytokine receptor γ chain leads to life-threatening, X-linked, severe combined immunodeficiency disease (XSCID) in humans, characterized by an extremely low number of T and NK cells.[48,49] These results suggest that NK cells are responsible for the formation of a progressively growing rapid large tumor and massive ascites of PEL cells in SCID mice at inoculation sites.

Severe combined immunodeficiency mice have NK cells, an important immune effector population implicated in protection against tumor metastasis and viral infection.[17,50] It has been reported recently that individuals with low natural cytotoxic activity of peripheral blood lymphocytes are at a significantly higher risk of cancer, compared with those of median or high activity, as well as functional impairment of NK cells in viral infection.[23] To assess the infiltration of PEL cells, we carried out histological examinations of tumor tissue and the different organs of mice inoculated with BCBL-1 cells (Fig. 3h). Infiltration of tumor cells was found in various organs of NOG mice inoculated with BCBL-1 cells. We found that NOD/SCID inoculated with BCBL-1 cells exhibited no infiltrate in any organs. NOD/SCID mice immunosuppressed by pretreatment with anti-NK antibody showed infiltration of PEL cells to a lesser extent in various organs of mice inoculated with BCBL-1 cells. HE and immunohistochemical staining showed a degree of infiltration of tumor cells in the lung of mice inoculated with BCBL-1 (Fig. 3h). These results suggest that NK cells play an important role in the infiltration of cancer cells in various organs.

Activated NK cells inhibit tumor growth and infiltration *in vivo*. As the above results suggested the potential role of NK cells in tumor growth and metastasis, we next examined whether adoptive transfer of activated NK cells could inhibit tumor growth and infiltration of xenografted PEL cells in the NOG mouse model. For this purpose, freshly isolated PBMC from the blood of healthy donors were cultured for 2–3 weeks to generate NK cells. NK cells were expanded *ex vivo* by several hundred to 2500-fold after 2 weeks cultivation and the expression level of CD69, an activated marker of NK cells, was increased dramatically. The purity of the activated NK cells used in the present study was 92–95% (data not shown). NK cells use cytoplasmic granules containing perforins and granzymes to kill the target cells. Using a highly sensitive flow cytometry-based intracellular cytokine assay, we next investigated the expression of intracellular perforins and granzymes in NK cells. Intracellular perforin and granzyme expression was increased in activated culture cells in comparison to freshly isolated cells from healthy donors (data not shown). PBMC, NK cell line KHYG-1 and activated NK cells were analyzed for cytotoxic activity against the NK-susceptible K562 erythroleukemia cell line (Fig. 4a,b). Cytotoxic activity of cells cultured for 2 weeks was increased significantly compared with freshly isolated PBMC from healthy donors (Fig. 4b). Activated NK cells also killed PEL cells efficiently *in vitro* at various E/T ratios, but the NK cell line KHYG-1 did not (Fig. 4c).

To examine the antitumor effect of activated NK cells against PEL, we injected the PEL cell line BCBL-1 (2×10^6) ip into the abdominal region of NOG mice. Three days after inoculation, mice were treated with either RPMI-1640 (as control) or activated NK cells (1×10^7) ip on days 4, 10 and 17. BCBL-1 cell inoculation promoted the development of massive ascites in the peritoneal cavity of all control mice within 3 weeks of inoculation. In contrast, activated NK-treated mice appeared to be

doi: 10.1111/j.1349-7006.2006.00319.x

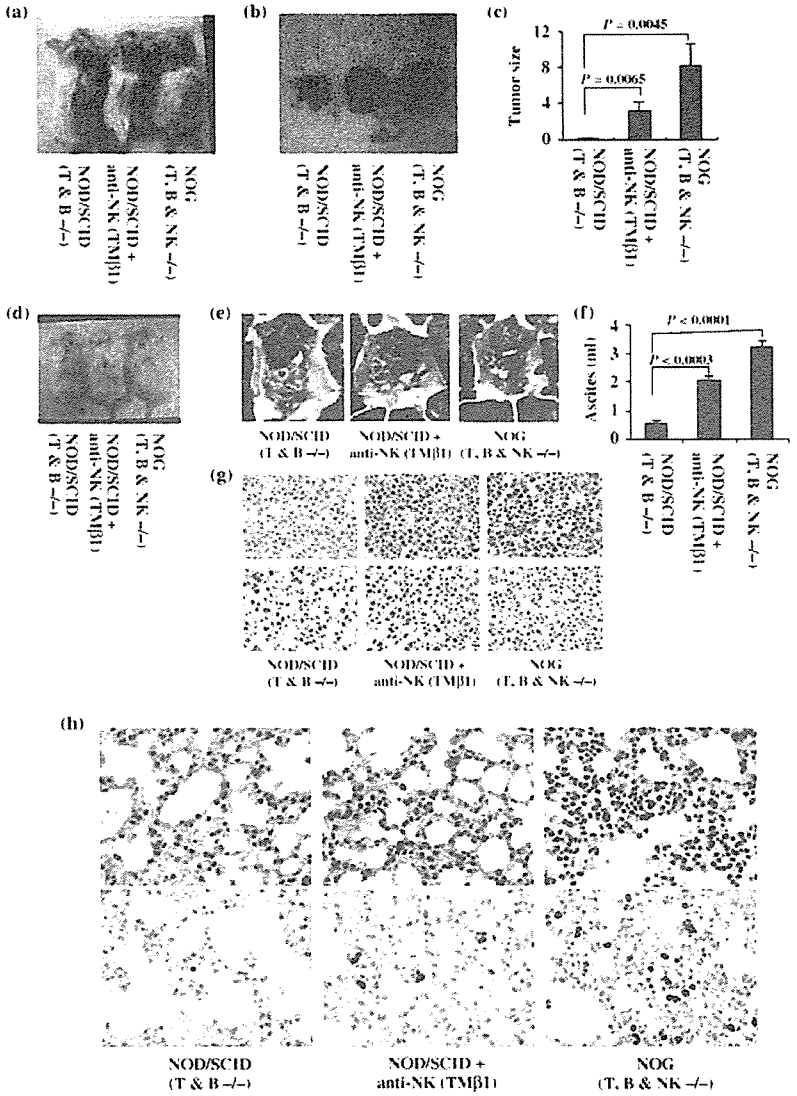

Fig. 3. Natural killer (NK) cells in tumor growth and infiltration. BCBL-1 cells were inoculated subcutaneously in the postauricular region or intraperitonealy in the abdominal region of T and B knock-out NOD/SCID, TMβ1-pretreated T and B knock-out NOD/SCID and T, B and NK knock-out NOG mice. (a) Photograph of mice inoculated with BCBL-1 cells subcutaneously in the postauricular region. (b) Photograph of BCBL-1 tumor 3 weeks formed subcutaneously after inoculation of cells. (c) Subcutaneous tumor size of mice inoculated with BCBL-1 cells, shown as the mean ± s.e.m. from six mice. Tumor size of TMβ1-pretreated NOD/SCID mice was significantly larger than NOD/SCID ($P = 0.0065$) and that of NOG mice was more significant than NOD/SCID ($P = 0.0045$). (d) Photograph of ascites-bearing mice inoculated with BCBL-1 cells intraperitonealy in the abdominal region. (e) Photograph of the peritoneal cavity of mice 3 weeks after inoculation of BCBL-1. Left, middle and right panels represent the T and B knock-out NOD/SCID, TMβ1-pretreated T and B knock-out NOD/SCID and T, B and NK knock-out NOG mice, respectively. Arrow head indicates the tumor in mice inoculated intraperitonealy. (f) Volume of ascites in mice inoculated with BCBL-1 cells, shown as the mean ± s.e.m. from six mice. Volume of ascites in TMβ1-pretreated NOD/SCID mice was significantly higher than NOD/SCID ($P = 0.0003$) and that of NOG mice was more significant than NOD/SCID ($P < 0.0001$). Hematoxylin–eosin (HE) and immunohistochemical staining of (g) lung tissue and (h) tumor tissue of BCBL-1-injected mice. Upper panels represent HE staining. Immunohistochemical staining was conducted using rabbit anti-LANA (lower panels). Left, middle and right panels represent results from T and B knock-out NOD/SCID, TMβ1-pretreated T and B knock-out NOD/SCID and T, B and NK knock-out NOG mice, respectively. Magnification, ×40.

healthy and had a significantly lower volume of ascites (Fig. 5a,b). Clinical evaluation of organ infiltration 3 weeks after injection of PEL cells showed that activated NK treatment inhibited their infiltration into the lung. In contrast, all control mice showed massive infiltration of tumor cells into the lung (Fig. 5c). Organ infiltration of tumor cells was analyzed and evaluated by HE and immunostaining of LANA. These data indicate that activated NK cells significantly inhibit the growth and infiltration of PEL cells *in vivo* (Fig. 5).

Discussion

Natural killer cells form a first line of defense against pathogens or host cells that are stressed or cancerous. To execute the concept of using activated NK cells in order to prevent cancer, it is indispensable to know how NK cells are important for tumor growth and infiltration. There have been a number of reports about the contribution of NK cells in tumor growth and metastasis. In particular, whole-body irradiation has been reported to suppress NK activity and increase the ability of human and murine tumors to be transplanted into SCID mice.[42–46] Treatment of mice with murine anti-NK antibody, which transiently inhibits NK-cell activity, results in efficient engraftment of tumor cells in SCID mice.[15,47] In the present study, we demonstrated the direct role of NK cells in tumor growth and metastasis using T, B and NK knock-out NOG and T and B knock-out NOD/SCID mice. PEL cells were able to produce a large tumor and massive ascites very efficiently at inoculated sites and infiltrate various organs in T, B and NK nock-out NOG mice. We found that T and B knock-out NOD/SCID mice inoculated with PEL cells formed small tumors and a lower volume of ascites, but completely failed to infiltrate. T and B knock-out NOD/SCID mice were further immunosuppressed by pretreatment with anti-NK antibody, which enhanced tumor and ascites formation as well as organ infiltration. These results demonstrate the critical role of NK cells in tumor growth and infiltration using NK knock-out mice. It is of particular importance that ip-inoculated PEL cells were found to form clinically relevant lymphomatous effusions in the peritoneal cavity and small tumor mass as well as infiltration. This clinically relevant

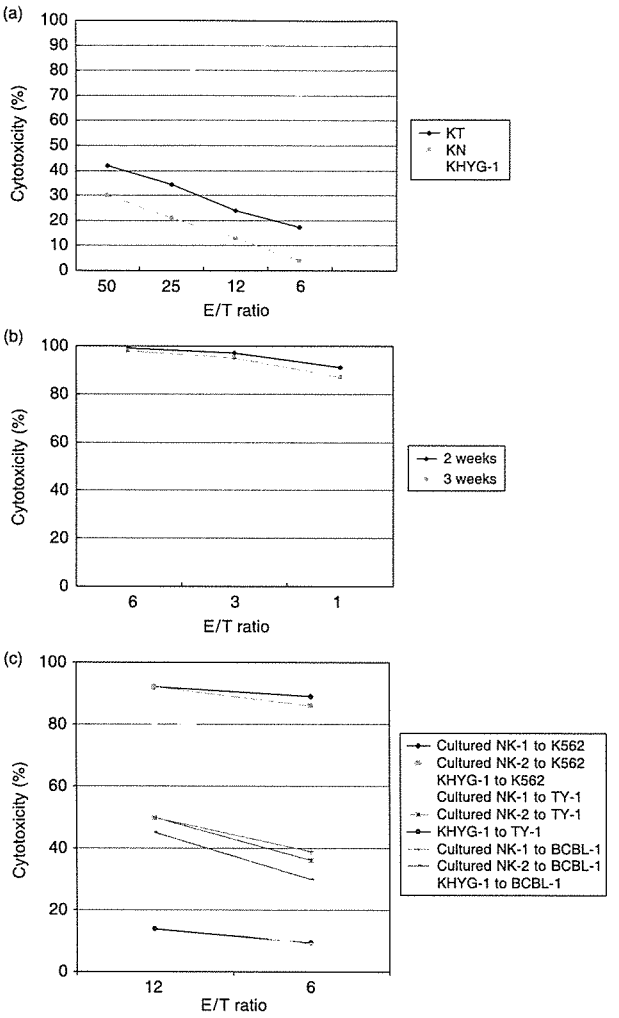

Fig. 4. Cytotoxic activity of activated natural killer (NK) *in vitro* culture cells. (a) Spontaneous cytotoxic activity of freshly isolated peripheral blood mononuclear cells (KT-1 and KN-2 represent samples from two donors) and NK cell line KHYG-1 against K-562 cells at different effector-to-target (E/T) ratios. (b) Cells cultured for 2 weeks against K-562 cells at different E/T ratios. (c) Cytotoxic activity of activated NK cells (NK-1 and NK-2 represent samples from two donors) against primary effusion lymphoma cells *in vitro* at various E/T ratios.

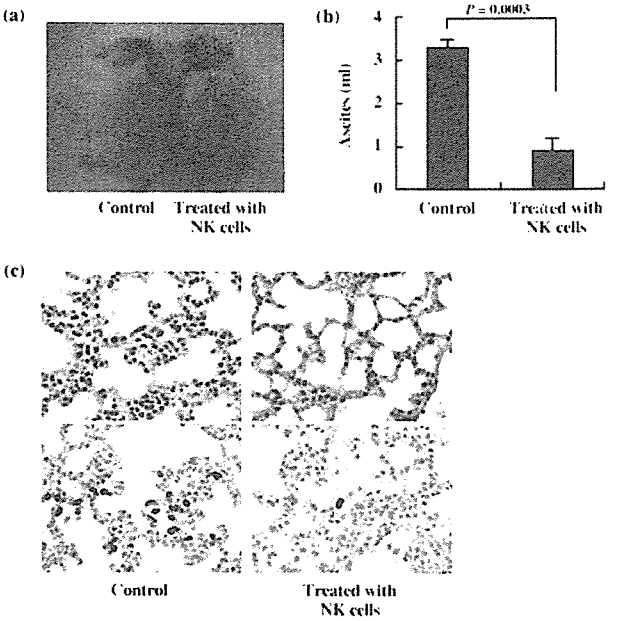

Fig. 5. Inhibition of primary effusion lymphoma (PEL) cell growth and infiltration in NOG mice. T, B and natural killer (NK) knock-out NOG mice were injected with PEL cells (2×10^6) intraperitonealy in the abdominal region. Mice were administered either RPMI-1640 or activated NK cells (1×10^7) intraperitonealy on days 4, 10 and 17 followed by observation for up to 3 weeks. (a) Photograph of ascites-bearing control PEL mice and activated NK-treated PEL mice. (b) Volume of ascites in control PEL mice and activated NK-treated PEL mice. Volume of ascites in mice inoculated with BCBL-1 cells, shown as the mean ± s.e.m. from six mice ($P = 0.0003$). (c) Hematoxylin–eosin (HE) and immunohistochemical staining of the lung of NOG mice 3 weeks after inoculation of PEL cells using anti-LANA. Upper and lower panels show HE and immunohistochemical staining, respectively. Left and right panels represent the data from control mice and mice treated with activated NK cells, respectively. Magnification, ×40. The data represent six mice in each group and three healthy donors (two mice for each donor).

animal model without changes in its histomorphology or tumor marker expression would be useful to understand and investigate the mechanism of PEL cell growth and infiltration.

In patients with cancer and viral infection, NK-cell function has been shown to be impaired, as determined by the reduced proliferation, response to interferon (IFN), and cytotoxicity of the cells of patients *ex vivo*.[51,52] In the present study, we inoculated activated NK cells to treat tumor-bearing mice to further clarify the role of NK cells in tumor growth and infiltration. Transfer of activated NK cells in T, B and NK knock-out NOG mice showed significant inhibition of tumor and ascites formation as well as infiltration. T, B and NK knock-out NOG mice treated with activated NK cells rejected the tumor cells to a similar extent as T and B knock-out NOD/SCID mice.

Natural killer cells kill target cells by various mechanisms. One way is by the release of cytoplasmic granules – complex organelles that combine specialized storage and secretory functions with the generic degradative functions of lysosomes. These granules contain a number of proteins, such as perforins and granzymes, which lyse target cells. Increased perforin and granzyme expression in activated NK cells was significantly correlated with inhibition of tumor growth and metastasis in the NOG mouse model. Perforin- and granzyme-mediated apoptosis is the principal pathway used by NK cells to eliminate tumor and virus-infected cells.[53] Studies in perforin-deficient mice have revealed that this protein is required for most NK-cell cytotoxicity.[54]

In summary, NK knock-out NOG mice were very efficient in the formation of primary tumors and organ infiltration. These results indicate that activated human NK cells prevent tumor growth and infiltration in NOG mice. Finally, our results suggest that NK cells play a critical role in tumor growth and infiltration, and that activated NK cells could be a promising immunotherapeutic strategy against cancer or viral infection either alone or in combination with conventional therapy. The reproducible growth behavior and preservation of characteristic features of PEL cells also suggest that the NOG mouse model system described in the present study may provide a novel opportunity to understand and investigate the mechanism of pathogenesis and malignant cell growth of PEL.

doi: 10.1111/j.1349-7006.2006.00319.x

Acknowledgments

We thank K. Ohba of the Department of Molecular Virology, S. Ichinose of the Instrumental Analysis Research Center and S. Endo of the Animal Research Center, Tokyo Medical and Dental University for their advice and assistance with the experiments. We also thank Y. Sato of the National Institute of Infectious Diseases for her excellent technical assistance. This work was supported by grants from the Ministry of Education, Science and Culture; the Ministry of Health, Labor and Welfare; and Human Health Science of Japan.

References

1 Jaffe ES, Harris NL, Stein H, Vardiman JW, eds. *World Health Organization Classification of Tumors, Pathology and Genetics of Tumors of Haematopoietic and Lymphoid Tissues*. Lyon, France: IARC Press, 2001.
2 Gaidano G, Carbone A. Primary effusion lymphoma: a liquid phase lymphoma of fluid-filled body cavities. *Adv Cancer Res* 2001; **80**: 115–46.
3 Cesarman E, Knowles DM. The role of Kaposi's sarcoma-associated herpesvirus (KSHV/HHV-8) in lymphoproliferative diseases. *Semin Cancer Biol* 1999; **9**: 165–74.
4 Klein U, Gloghini A, Gaidano G *et al.* Gene expression profile analysis of AIDS-related primary effusion lymphoma (PEL) suggests a plasmablastic derivation and identifies PEL-specific transcripts. *Blood* 2003; **102**: 4115–21.
5 Cesarman E, Chang Y, Moore PS, Said JW, Knowles DM. Kaposi's sarcoma-associated herpesvirus-like DNA sequences in AIDS-related body-cavity-based lymphomas. *N Engl J Med* 1995; **332**: 1186–91.
6 Horenstein MG, Nador RG, Chadburn A *et al.* Epstein–Barr virus latent gene expression in primary effusion lymphomas containing Kaposi's sarcoma-associated herpesvirus/human herpesvirus-8. *Blood* 1997; **90**: 1186–91.
7 Nador RG, Cesarman E, Chadburn A *et al.* Primary effusion lymphoma: a distinct clinicopathologic entity associated with the Kaposi's sarcoma-associated herpes virus. *Blood* 1996; **88**: 645–56.
8 Schmidt M, Deschner EE, Thaler HT, Clemments L, Good RA. Gastrointestinal cancer studies in the human to nude mouse heterotransplant system. *Gastroenterology* 1977; **72**: 829–37.
9 Bosma GC, Custer RP, Bosma MJ. A severe combined immunodeficiency mutation in the mouse. *Nature* 1983; **301**: 527–30.
10 Schuler W, Bosma MJ. Nature of the scid defect: a defective VDJ recombinase system. *Curr Top Microbiol Immunol* 1989; **152**: 55–62.
11 Kamel-Reid S, Letarte M, Sirard C *et al.* A model of human acute lymphoblastic leukemia in immune-deficient SCID mice. *Science* 1989; **246**: 1597–600.
12 Mosier DE, Gulizia RJ, Baird SM, Wilson DB. Transfer of a functional human immune system to mice with severe combined immunodeficiency. *Nature* 1988; **335**: 256–9.
13 Ito M, Hiramatsu H, Kobayashi K *et al.* NOD/SCID/γc^{null} mouse: An excellent recipient mouse model for engraftment of human cells. *Blood* 2002; **100**: 3175–82.
14 Dorshkind K, Pollack SB, Bosma MJ, Phillips RA. Natural killer (NK) cells are present in mice with severe combined immunodeficiency (scid). *J Immunol* 1985; **134**: 3798–801.
15 Feuer G, Stewart SA, Baird SM, Lee F, Feuer R, Chen ISY. Potential role of natural killer cells in controlling tumorigenesis by human T-cell leukemia Viruses. *J Virol* 1994; **69**: 1328–33.
16 Welsh RM. Regulation of virus infections by natural killer cells: a review. *Nat Immun Cell Growth Regul* 1986; **5**: 169–99.
17 Trinchieri G. Biology of natural killer cells. *Adv Immunol* 1989; **47**: 187–376.
18 Moretta A. Natural killer cells and dendritic cells: rendezvous in abused tissues. *Nat Rev Immunol* 2002; **2**: 957–64.
19 Raulet DH. Interplay of natural killer cells and their receptors with the adaptive immune response. *Nat Immunol* 2004; **5**: 996–1002.
20 Karre K, Ljungger HG, Piontek G, Kiessling R. Selective rejection of H-2-deficient lymphoma variants suggests alternative immune defense strategy. *Nature* 1986; **319**: 675–8.
21 Pena J, Alonso C, Solana R, Serrano R, Carracedo J, Ramirez R. Natural killer susceptibility is independent of HLA class I antigen expression on the cell lines obtained from human solid tumors. *Eur J Immunol* 1990; **20**: 2445–9.
22 Litwin V, Gumperz J, Parham P, Philips JH, Lanier LL. Specificity of HLA class I antigen recognition by human NK clones: evidence for clonal heterogeneity, protection by self and non-self alleles, and influence of the target cell type. *J Exp Med* 1993; **178**: 1321–36.
23 Imai K, Matsuyama S, Miyake S, Suga K, Nakachi K. Natural cytotoxic activity of peripheral-blood lymphocytes and cancer incidence: an 11-year follow-up study of a general population. *Lancet* 2000; **356**: 1795–9.
24 Ullum H, Gotzsche PC, Victor J, Dickmeiss E, Skinhoj P, Pedersen BK. Defective natural immunity: an early manifestation of human immunodeficiency virus infection. *J Exp Med* 1995; **182**: 789–99.
25 Ahmad R, Menezes J. Defective killing activity against gp120/41-expressing human erythroleukaemic K562 cell line by monocytes and natural killer cells from HIV-infected individuals. *AIDS* 1996; **10**: 143–9.
26 Scott-Algara D, Paul P. NK cells and HIV infection: lessons from other viruses. *Curr Mol Med* 2002; **2**: 757–68.
27 Bonaparte MI, Barker E. Inability of natural killer cells to destroy autologous HIV-infected T lymphocytes. *AIDS* 2003; **17**: 487–94.
28 Sirianni MC, Libi F, Campagna M *et al.* Downregulation of the major histocompatibility complex class I molecules by human herpesvirus type 8 and impaired natural killer cell activity in primary effusion lymphoma development. *Br J Haematol* 2005; **130**: 92–5.
29 Sirianni MC, Vincenzi L, Topino S *et al.* NK cell activity controls human herpesvirus 8 latent infection and is restored upon highly active antiretroviral therapy in AIDS patients with regressing Kaposi's sarcoma. *Eur J Immunol* 2002; **32**: 2711–20.
30 Lanier LL. NK cell receptors. *Annu Rev Immunol* 1998; **16**: 356–93.
31 Moretta A, Bottino C, Mingari MC, Biassoni R, Moretta L. What is a natural killer cell? *Nat Immunol* 2002; **3**: 6–8.
32 Koo GC, Dumont FJ, Tutt M, Hackett J Jr, Kumar V. The NK-1.1(–) mouse: a model to study differentiation of murine NK cells. *J Immunol* 1986; **137**: 3742–7.
33 Smyth MJ, Crowe NY, Godfrey DI. NK cells and NKT cells collaborate in host protection from methylcholanthrene-induced fibrosarcoma. *Int Immunol* 2001; **13**: 459–63.
34 Smyth MJ, Godfery DI, Trapani JA. A fresh look at tumor immunosurveillance and immunotherapy. *Nature* 2001; **2**: 293–9.
35 Dewan MZ, Terashima K, Taruishi M *et al.* Rapid tumor formation of human T-cell leukemia virus type 1-infected cell lines in novel NOD-SCID/γc^{null} mice: suppression by an inhibitor against NF-κB. *J Virol* 2003; **77**: 5286–94.
36 Dewan MZ, Uchihara JN, Terashima K *et al.* Efficient intervention of growth and infiltration of primary adult T-cell leukemia cells by an HIV protease inhibitor, ritonavir. *Blood* 2006; **107**: 716–24.
37 Renne R, Zhong W, Herndier B *et al.* Lytic growth of Kaposi's sarcoma-associated herpesvirus (human herpesvirus 8) in culture. *Nat Med* 1996; **2**: 342–6.
38 Katano H, Hoshino Y, Morishita Y *et al.* Establishing and characterizing a CD30-positive cell line harboring HHV-8 from a primary effusion lymphoma. *J Med Virol* 1999; **58**: 394–401.
39 Katano H, Sato Y, Kurata T, Mori S, Sata T. High expression of HHV-8-encoded ORF73 protein in spindle-shaped cells of Kaposi's sarcoma. *Am J Pathol* 1999; **155**: 47–52.
40 Dorshkind K, Pollack SB, Bosma MJ, Phillips RA. Natural killer (NK) cells are present in mice with severe combined immunodeficiency (scid). *J Immunol* 1985; **134**: 3798–801.
41 Visonneau S, Cesano A, Torosian MH, Miller EJ, Santoli D. Growth characteristics and metastatic properties of human breast cancer xenografts in immunodeficient mice. *Am J Pathol* 1998; **152**: 1299–311.
42 Cavacini LA, Giles-Komar J, Kennel M, Quinn A. Effect of immunosuppressive therapy on cytolytic activity of immunodeficient mice: implications for xenogeneic transplantation. *Cell Immunol* 1992; **144**: 296–310.
43 Hochman PS, Cudkowicz G, Dausset J. Decline of natural killer cell activity in sublethally irradiated mice. *J Natl Cancer Inst* 1978; **61**: 265–8.
44 Huang YW, Richardson JA, Tong AW, Zhang BQ, Stone MJ, Vitetta ES. Disseminated growth of a human multiple myeloma cell line in mice with severe combined immunodeficiency disease. *Cancer Res* 1993; **53**: 1392–6.
45 Lapidot T, Sirard C, Vormoor J *et al.* A cell initiating human acute myeloid leukaemia after transplantation into SCID mice. *Nature* 1994; **367**: 645–8.
46 Taghian A, Budach W, Zietman A, Freeman J, Gioioso D, Suit HD. Quantitative comparison between the transplantability of human and murine tumors into the brain of NCr/Sed-nu/nu nude and severe combined immunodeficient mice. *Cancer Res* 1993; **53**: 5018–21.
47 Tanaka T, Tsudo M, Karasuyama H *et al.* Novel monoclonal antibody against murine IL-2 receptor beta-chain: Characterization of receptor expression in normal lymphoid cells and EL-4 cells. *J Immunol* 1991; **147**: 2222–8.
48 Noguchi M, Yi H, Rosenblatt HM *et al.* Interleukin-2 receptor gamma chain mutation results in X-linked severe combined immunodeficiency in humans. *Cell* 1993; **73**: 147–57.
49 Puck JM, Deschenes SM, Porter JC *et al.* The interleukin-2 receptor gamma chain maps to Xq13.1 and is mutated in X-linked severe combined immunodeficiency, SCIDX1. *Hum Mol Genet* 1993; **2**: 1099–104.
50 Welsh RM. Regulation of virus infections by natural killer cells: a review. *Nat Immun Cell Growth Regul* 1986; **5**: 169–99.
51 Whiteside TL, Herberman RB. Role of human natural killer cells in health and disease. *Clin Diagn Laboratory Immunol* 1994; **1**: 125–33.
52 Whiteside TL, Vujanovic NL, Herberman RB. Natural killer cells and tumor therapy. *Curr Top Microbiol Immunol* 1998; **230**: 221–44.
53 Trapani JA, Davis J, Sutton VR, Smyth MJ. Proapoptotic functions of cytotoxic lymphocyte granule constituents *in vitro* and *in vivo*. *Curr Opin Immunol* 2000; **12**: 323–9.

Available online at www.sciencedirect.com
SCIENCE DIRECT
ELSEVIER
Virology 352 (2006) 100–109
VIROLOGY
www.elsevier.com/locate/yviro

Expression of Kaposi's sarcoma-associated herpesvirus-encoded K10/10.1 protein in tissues and its interaction with poly(A)-binding protein

Takayuki Kanno, Yuko Sato, Tetsutaro Sata, Harutaka Katano *

Department of Pathology, National Institute of Infectious Diseases, 1-23-1 Toyama, Shinjuku-ku, Tokyo 162-8640, Japan

Received 12 December 2005; returned to author for revision 6 January 2006; accepted 5 April 2006
Available online 22 May 2006

Abstract

The K10/10.1 protein is encoded by a cluster of interferon regulatory factor (IRF) homologues in the Kaposi's sarcoma-associated herpesvirus (KSHV, human herpesvirus 8, HHV-8) genome. In the present study, we showed that an anti-K10 antibody reacted with a 110-kDa protein encoded by the K10/10.1 gene of KSHV in KSHV-infected primary effusion lymphoma (PEL) cell lines. Expression of K10/10.1 protein was induced by phorbol ester in KSHV-infected cells. A reporter gene assay demonstrated that K10/10.1 protein did not influence promoter activity of human interferon genes, regardless of its homology to human IRFs. Poly(A)-binding protein (PABP) was identified as a partner of K10/10.1 protein. Immunoprecipitation revealed that K10/10.1 protein interacted with PABP specifically in PEL cell lines. IFA revealed co-localization of K10/10.1 protein and PABP in the nucleus of KSHV-infected cells. These data suggest that K10/10.1 protein may affect the translational status or stability of mRNA in host cells.

Keywords: Kaposi's sarcoma-associated herpesvirus (KSHV/HHV-8); K10/10.1; Kaposi's sarcoma (KS); Multicentric Castleman's disease (MCD); Poly(A)-binding protein (PABP); Primary effusion lymphoma (PEL)

Introduction

Kaposi's sarcoma-associated herpesvirus (KSHV, human herpesvirus 8, HHV-8) is associated with the pathogenesis of KS, primary effusion lymphoma (PEL), and multicentric Castleman's disease (MCD) (Moore and Chang, 2001). One of the unique characteristics of this virus is that it encodes several homologues of human cytokines, cell cycle-associated genes, and chemokines. Among them, KSHV contains a cluster of interferon regulatory factor (IRF)-encoded genes in its genome. At least 7 homologues of IRFs have been identified in this cluster, i.e., K9 (viral IRF-1 or vIRF-1), K10, K10.1 (vIRF-4), K10.5 (vIRF-3 or LANA2), K10.7, K11, and vIRF2 (Afonina et al., 1998; Burysek et al., 1999; Cunningham et al., 2003; Lubyova and Pitha, 2000; Rivas et al., 2001). Some of these IRF homologues have been previously investigated, and their functions have been reported. vIRF-1 was found to have a similar function to human IRF-2 (hIRF-2) (Burysek et al., 1999; Li et al., 1998; Pozharskaya et al., 2004; Zimring et al., 1998). Like hIRF-2, vIRF-1 suppresses type I-interferon promoter activity and IFN-stimulated activation of IFN-stimulated gene (ISG) promoters (Afonina et al., 1998; Burysek et al., 1999; Zimring et al., 1998). vIRF-1 is also involved in oncogenesis by binding cellular p53 and CBP/p300 (Burysek et al., 1999). vIRF-2 suppresses interferon promoter activity and binds to IRF-1, IRF-2, ICSBP, and CBP (Burysek and Pitha, 2001; Burysek et al., 1999). vIRF-2 interacts with double-stranded RNA-activated protein kinase and inhibits antiviral effects of interferon (Burysek and Pitha, 2001). vIRF-3 (LANA2) is unique among vIRFs (Lubyova et al., 2004; Lubyova and Pitha, 2000; Rivas et al., 2001). Its kinetics are those of the latent proteins, and almost all KSHV-infected B-cells express vIRF-3 in their nucleus (Rivas et al., 2001). Moreover, vIRF-3 inhibits p53-dependent apoptosis by binding to p53 and CBP/p300, suggesting that vIRF-3 plays an important role in pathogenesis of malignancies with a latent infection with KSHV (Lubyova et al., 2004; Rivas et al., 2001). Thus, KSHV-encoded IRFs show

* Corresponding author. Fax: +81 3 5285 1189.
E-mail address: katano@nih.go.jp (H. Katano).

0042-6822/$ - see front matter © 2006 Elsevier Inc. All rights reserved.
doi:10.1016/j.virol.2006.04.009

various functions, and their expression varies among genes. On the other hand, other vIRFs, e.g., K10, K11, vIRF4 (K10.1), and K10.7, have been poorly characterized, and their functions are still unknown (Cunningham et al., 2003). We previously showed that expression of K10 protein was induced by 12-*O*-tetradecanoylphorbol-13-acetate (TPA) in the KSHV-infected PEL cell lines, suggesting that K10 protein belonged to a family of lytic proteins (Katano et al., 2000b). Histologically, K10 protein is expressed in the nucleus by very few tumor cells in Kaposi's sarcoma (KS) tissues, although a small number of mantle zone B cells express K10 protein in their cytoplasm in multicentric Castleman's disease (MCD) tissues (Katano et al., 2000b). Furthermore, the length of ORF K10 gene is more than 2 kbp, which makes it the longest gene among all vIRFs (Cunningham et al., 2003). Transcriptional analysis revealed that ORF K10 was transcribed with ORF K10.1 as a fusion gene (K10/10.1 gene) (Cunningham et al., 2003; Jenner et al., 2001). Even though a part of the K10 gene is homologous to hIRFs, a large part of it does not correspond to any other human genes. Therefore, we hypothesized that K10/10.1 protein, a product of K10/10.1 gene, had other functions besides those of IRFs. In the present study, we revealed that the K10/10.1 transcript produced a 110-kDa protein (K10/10.1 protein), and we identified poly (A)-binding protein as a binding partner of the K10/10.1 protein.

Results

Cloning of the K10/10.1 transcript from a cDNA library

To identify transcripts encoded by the K10 gene, we immunoscreened a cDNA library. When 1×10^6 clones of a cDNA library constructed from TY-1 cells were screened using the anti-K10 polyclonal antibody (Katano et al., 2000b), 8 positive clones were obtained. Sequence analysis revealed that these clones consisted of 3 groups. The first group contained a 2921-bp cDNA with a poly(A) signal sequence corresponding to the K10/10.1 transcript (Jenner et al., 2001). The 2 other clone groups were shorter than the K10/10.1 group, and only coded for the K10 gene characterized as a 2281-bp fragment (bases 88,286–86,006 of GenBank acc. no. U75698) or a 2080-bp fragment (bases 88,085–86,006 of GenBank acc. no. U75698). To confirm expressions of these three forms of K10 transcripts, we performed Northern blot hybridization using the K10 gene as a probe. Northern blotting demonstrated that two bands were induced in TY-1 cells with TPA stimulation (Fig. 1A). The size of the longest band was 2.9 kb, possibly corresponding to the K10/10.1 transcript (Jenner et al., 2001). No band was found at 2281 and 2080 b. In addition to the band of the K10/10.1 transcript, a strong 1.0-kb band was observed in stimulated PEL cells, suggesting the presence of another form of the K10 gene. Unstimulated PEL cells demonstrated two

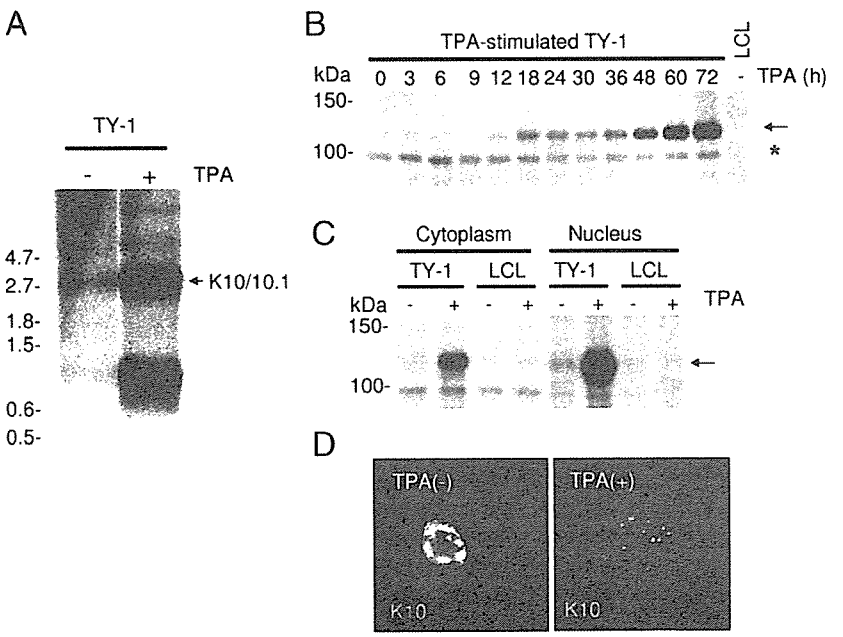

Fig. 1. Expression of K10/10.1 gene and protein in a PEL cell line. (A) Northern blot hybridization. mRNAs extracted from TPA-stimulated TY-1 (+) or unstimulated TY-1 (−) cells were electrophoresed and blotted on a membrane. Radiolabeled K10 DNA (amplified by PCR) was used as probe. The arrow indicates the K10/10.1 gene transcript. The lower band at 1.0 kb represents another transcript of the K10 gene. (B) Western blot analysis for K10/10.1 protein in TPA-stimulated TY-1 cells. Numbers of hours after addition of TPA are shown at the top of the panel. LCL: lymphoblastoid cell line as a negative control. The arrow indicates specific bands obtained with the anti-K10 rabbit polyclonal antibody, while lower bands (asterisk) are non-specific. (C) Western blot analysis for K10/10.1 protein in subcellular fractions. The arrow indicates K10/10.1 protein-specific bands. (D) IFA of K10/10.1 protein in unstimulated (left) and TPA-stimulated TY-1 (right) cells using anti-K10 rabbit polyclonal antibody. K10/10.1 protein is represented in green color. The red color indicates nuclear counterstaining with propidium iodide.

weak bands at 2.9 kb and 1.0 kb. Thus, we concluded that a 2.9-kb transcript of K10/10.1 was the major transcript of the K10/10.1 gene, and that 2 other short clone groups were artificially present.

Expression and kinetics of K10/10.1 gene/protein in PEL cell lines

Several studies reported kinetics of KSHV-encoded genes in PEL cell lines (Fakhari and Dittmer, 2002; Jenner et al., 2001; Sun et al., 1999). We previously demonstrated that K10 protein was induced by TPA, suggesting that K10 protein was a lytic protein (Katano et al., 2000b). DNA array analysis by another group suggested the presence of 2 transcripts including the K10 gene, i.e., K10/10.1 and K10 (Jenner et al., 2001). Cluster analysis and RT-PCR suggested that K10 might be a latent gene, whereas K10/10.1 was a lytic gene (Jenner et al., 2001). Thus, we examined expressions of K10/10.1 gene and protein in PEL cell lines. Northern blot analysis demonstrated that K10/10.1 transcript (2.9 kb) was induced by TPA in TY-1 cells (Fig. 1A). Western blotting demonstrated that an anti-K10 antibody reacted with a 110-kDa protein of K10/10.1, and that amount of K10/10.1 protein increased after addition of TPA (Fig. 1B). Subcellular fractionation revealed that K10/10.1 protein was expressed mainly in the nucleus, and partly in the cytoplasm (Fig. 1C). IFA using anti-K10 antibody showed that K10/10.1 protein was expressed in the nucleus of a very small population of unstimulated PEL cells (Fig. 1D). When stimulated with TPA, the number of K10/10.1-positive cells increased. Dot-like signals were observed not only in the nucleus, but also in the cytoplasm of TPA-stimulated TY-1 cells (Fig. 1D). In addition, most of K10/10.1-positive cells expressed K10/10.1 protein in the nucleus, while some cells expressed K10/10.1 both in the cytoplasm and the nucleus. We also examined another KSHV-infected PEL cell line, BCBL-1, and obtained similar results (data not shown).

Expression of K10/10.1 protein in KS, MCD, and KSHV-associated solid lymphoma

We previously developed a polyclonal antibody to K10 protein, and reported expression of K10 protein in KS and MCD tissues (Katano et al., 2000b). As we showed in Fig. 1, Western blot analysis revealed that this anti-K10 antibody reacted with K10/10.1 protein predominantly (Fig. 1). In order to further reveal the detailed expression of K10/10.1 protein in KSHV-associated diseases, we performed immunohistochemistry for K10/10.1 protein in additional cases of KS, MCD, and in an animal model of KSHV-associated solid lymphoma (Katano et al., 2000b). As it was previously reported (Katano et al., 2000b),

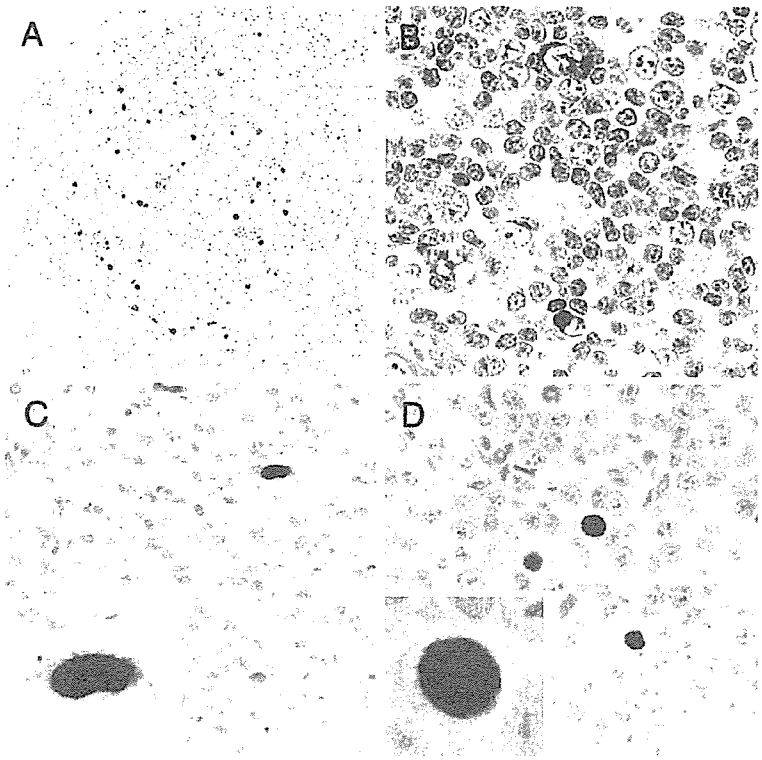

Fig. 2. Immunohistochemistry of K10/10.1 protein in KSHV-associated diseases. (A and B) Lymph node from a patient with MCD. The low power view shows K10/10.1 protein-positive cells in the mantle zone of the germinal center in a MCD lesion (A). Some B cells in the mantle zone show positive signals in the cytoplasm (B). (C) Kaposi's sarcoma (KS). One cell expresses K10/10.1 protein in this panel. In the high power view, diffuse staining is present in the nucleus (inset). (D) An animal model of KSHV-associated solid lymphoma. Some of the lymphoma cells are positive for K10/10.1 protein. In the high power view, the signal is seen as a dot-like staining pattern in the nucleus (inset).

we found that K10/10.1 protein was expressed predominantly in the cytoplasm of B cells in the mantle zone of MCD lesions (Figs. 2A and B). Expression of K10/10.1 protein was observed in the nucleus of KS cells, and the frequency of K10/10.1-positive cells was very low (less than 1%) in KS lesions (Fig. 2C). In an animal model of KSHV-associated solid lymphoma, K10/10.1 protein was expressed in the nucleus of lymphoma cells (Fig. 2D). A careful observation revealed that staining with the anti K10 antibody showed a dot-like pattern in the nucleus (Fig. 2D, inset).

Localization of K10/10.1 in transfectants

To investigate function and expression of K10/10.1 protein, we constructed a plasmid expressing K10/10.1 protein. A transfection study demonstrated that the expression plasmid produced a 110-kDa protein that reacted with anti-K10 antibody in 293T cells (Fig. 3A). IFA revealed its subcellular localization in K10/10.1-transfected HeLa cells (Fig. 3B). While K10/10.1 protein was expressed predominantly in the nucleus in 30% of transfectants, 60% of transfected cells expressed K10/10.1 protein in both the cytoplasm and nucleus, and the remaining 10% of cells showed K10/10.1 protein predominantly in the cytoplasm. We next constructed GFP-tagged plasmids expressing the K10/10.1 protein, and transfected them into HeLa cells (Fig. 3C). Similar localization was observed in the GFP-K10/10.1-transfected HeLa cells. Although PROSITE, an online protein domain searchable database (http://us.expasy.org/prosite/), did not detect any putative sequence of nuclear localization signals in the K10/10.1 gene, our data suggested that K10/10.1 might have unknown nuclear localization signals or DNA binding domains.

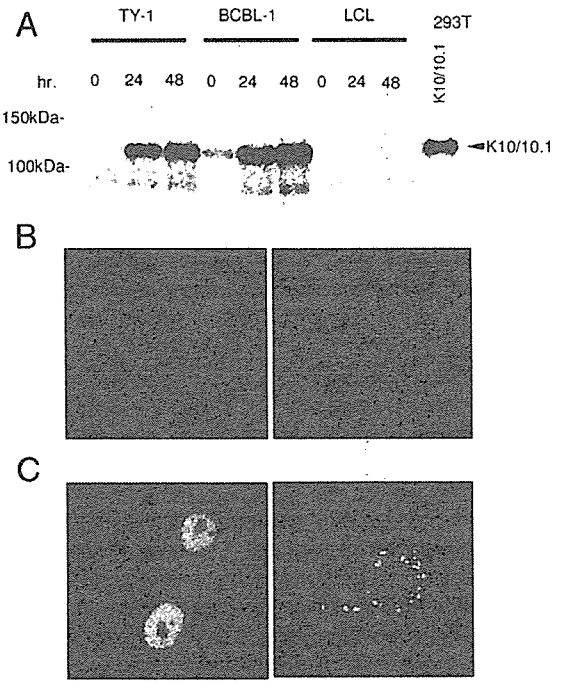

Fig. 3. Expression of K10/10.1 transcript in transfectants. (A) Western blot analysis. In 293T transfectants, the K10/10.1 transcript produced a protein with a similar size to that of K10/10.1 proteins in KSHV-infected PEL cell lines. (B) Localization of each form of K10 proteins in HeLa cells. The red color indicates K10/10.1 protein, and the blue color is the nucleus (TOPRO3). K10/10.1 protein is present predominantly in the nucleus (left panel) and rarely in the cytoplasm (right panel). (C) Localization of GFP-K10/10.1 protein in HeLa cells. GFP signal is observed predominantly in the nucleus (left panel), sometimes in both the cytoplasm and nucleus (right panel).

Functions as a homologue of IRFs

Since the K10/10.1 transcript is encoded in the cluster of vIRFs in KSHV genome, we compared the K10/10.1 protein with IRFs using multiple sequence alignments with the Clustal X software. Multiple sequence alignments demonstrated that K10.1 (the N-terminal region of the K10/10.1 protein) coded homologous regions to the DNA binding domain of IRFs, including a tryptophan pentad repeat (Fig. 4A). The N-terminus of the K10 protein, which localized in a middle part of K10/10.1 protein, also showed homologous regions to the DNA binding domain of IRFs. Moreover, K10/10.1 protein has some homologous regions in its C-terminus. A phylogenic tree analysis revealed that both K10 and K10.1 belonged to the same cluster as vIRF-1, suggesting that K10/10.1 protein might have similar functions to IRFs (Fig. 4B).

IFA demonstrated a dot-like staining pattern in the nucleus of PEL cell lines (Fig. 1D). It is known that vIRF-1 localizes in the promyelocytic leukemia protein (PML) bodies in the nucleus (Pozharskaya et al., 2004). Since K10/10.1 protein has a homology to vIRF-1, we investigated whether K10/10.1 protein co-localized with the PML bodies. IFA demonstrated that staining of K10/10.1 protein only partially overlapped with that of PML (Fig. 4C). Some hIRFs co-localize with the SC35 domain, a component in the nucleus close to the PML bodies (Maul, 1998). Therefore, we investigated if K10/10.1 protein co-localized with SC35. IFA revealed that signals of K10/10.1 protein overlapped with those of SC35 (Fig. 4D), suggesting that K10/10.1 protein was expressed in the SC35 domain near the PML body in the nucleus.

We then examined if K10/10.1 protein suppressed promoter activity of interferons. A reporter gene assay using pGL3-IFNB-Luc demonstrated that K10/10.1 protein did not suppress promoter activity of IFNB induced by a Sendai virus infection (Fig. 4E). These data suggested that K10/10.1 protein might not suppress promoter activity of IFNs, while K10/10.1 protein shows some homology with IRFs.

PABP binds to K10/10.1 protein

To further clarify the function of K10/10.1 protein, we next investigated its binding protein. GST-K10 fusion protein was mixed with TY-1 cell lysate, and a GST pull down assay was performed. SDS-PAGE of the pulled down proteins demonstrated the presence of a protein that specifically bound to K10 protein but not to GST in the TY-1 lysate (Fig. 5A). We excised the appropriate band from the gel, and analyzed it using matrix-

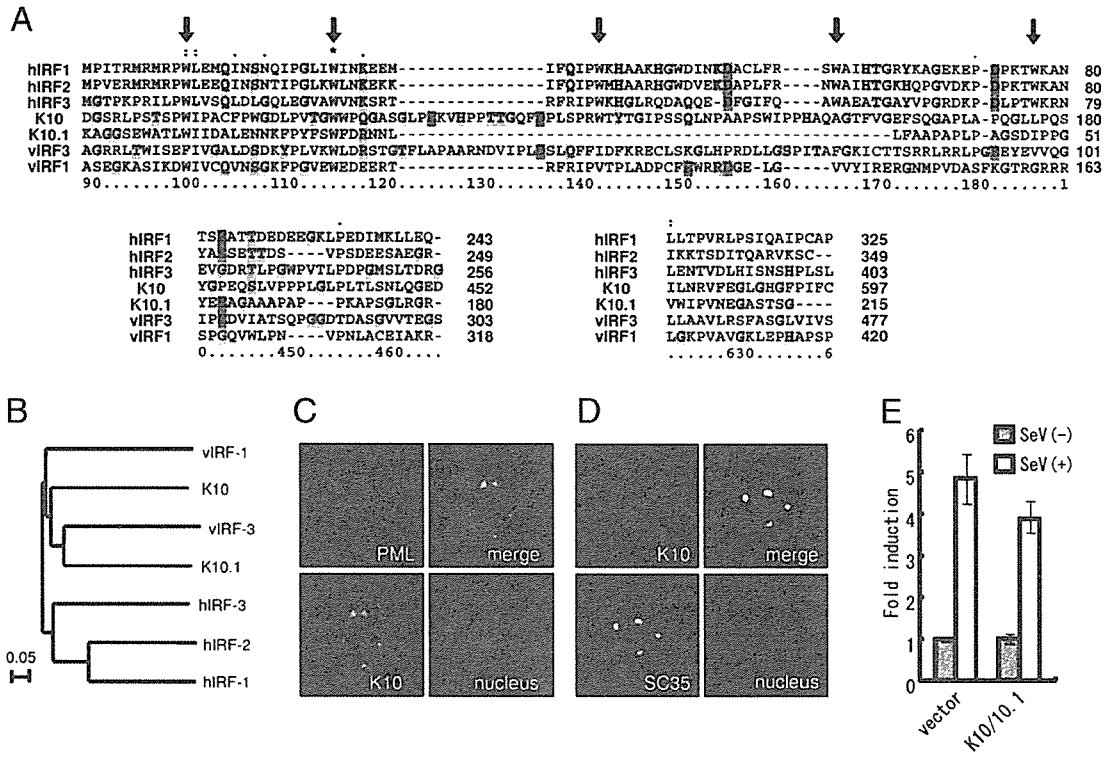

Fig. 4. K10/10.1 protein shows homologous domains to human and viral IRFs, but does not inhibit interferon promoter. (A) Alignment with IRFs using the Clustal X software. hIRF-1 (GenBank accession no. 87992), hIRF-2 (539621), hIRF-3 (4504725), vIRF-3 (AY008303), K10.1 (from 88410 to 88910 of KSU75698), K10 (from 86074 to 88164 of KSU75698), and vIRF-1 (4929348) were aligned. Arrows indicate tryptophan pentad repeats of the DNA binding domain. Numbers in the right of each panel indicate amino acids of each protein. Numbers counted automatically by the Cluster X were shown in the bottom of each panel. (B) Phylogenic tree analysis of IRFs, K10 and K10.1 proteins. The length of each branch indicates genetic distance with a scale size of 0.05 (5%). (C) Immunofluorescence of K10/10.1 protein and PML in TPA-stimulated TY-1 cells. PML and K10/10.1 protein were stained with Alexa 568 (red, upper left panel) and Alexa 488 (green, lower left panel), respectively. The nucleus was counterstained with TOPRO3 (blue, lower right panel). In the merged image (upper right), overlapping of the three colors is shown in white color. (D) Immunofluorescence of K10/10.1 protein and SC35 in TPA-stimulated TY-1 cells. (E) Reporter gene assay of IFNB promoter. The pGL3-IFNB-Luc reporter plasmid was co-transfected into HeLa cells with pBK-CMV vector (vector) and K10/10.1 expression plasmids. Cells were infected with Sendai virus 24 h after transfection, for 16 h, and analyzed for Luc activity. Error bars show standard deviation for triplicate experiments.

assisted laser desorption ionization/time-of-flight (MALDI-ToF) mass analysis. Mass spectrometry revealed that the protein corresponded to human poly(A)-binding protein (PABP), cytoplasmic 1. To confirm the binding of PABP to GST-K10 protein, we performed immunoblot analysis of the lysate obtained in the GST pull down (Fig. 5B). PABP was detected in the lysate pulled down with GST-K10 protein in the TY-1 lysate. In addition, Western blotting demonstrated that PABP was detected in the lysate immunoprecipitated with anti-K10 antibody in TY-1 and BCBL-1 cells (Fig. 5C). Moreover, K10/10.1 protein was detected in the lysate immunoprecipitated with anti-PABP antibody in cells (Fig. 5D). These data suggested that PABP bound to K10/10.1 protein in KSHV-infected PEL cells. To identify the binding site of PABP in K10/10.1 protein, we constructed plasmids expressing various deletion mutants of K10/10.1 protein (Fig. 6A). Immunoprecipitation clearly demonstrated that PABP bound to a 157–380 amino acid region of K10/10.1 protein (Fig. 6B). Finally, we investigated co-localization of PABP and K10/10.1 protein in KSHV-infected cells. In KSHV-infected PEL cells, TPA-stimulation induced K10/10.1 expression in the nucleus and cytoplasm (Fig. 1D). Interestingly, IFA revealed that PABP co-localized with K10/10.1 protein predominantly in the nucleus, but not in the cytoplasm (Fig. 7). Furthermore, in the nucleus of some cells, both K10/10.1 protein and PABP showed dot-like staining patterns, and co-localized in these dots. Since PABP localizes in the SC35 domain close to the PML bodies, and binds to poly(A) RNA in the nucleus (Afonina et al., 1998), these data suggested that K10/10.1 protein and PABP co-localized in the SC35 domain of TY-1 cells, and K10/10.1 protein might play a role in the function of PABP in the nucleus of KSHV-infected cells.

Discussion

In the present study, we characterized KSHV-encoded K10/10.1 protein. Our results showed that K10/10.1 protein was rarely expressed in the nucleus of KS cells, but was frequently found in the cytoplasm of the mantle zone B cells in MCD lesions. While functions of K10/10.1 protein are still unclear, K10/10.1 protein was identified as the longest homologue to

vIRFs, and its gene contained long sequences with no homology to IRFs. Thus, it is possible that K10/10.1 protein may have different functions from those of other vIRFs or hIRFs. Specifically, we showed that K10/10.1 protein did not influence promoter activity of interferons, and binding of K10/10.1 protein to PABP suggested that K10/10.1 protein affected host translation. Thus, K10/10.1 protein may play a different role from those of other viral IRFs in KSHV pathogenesis, while the K10/10.1 gene is encoded in the cluster of viral IRFs.

Although KSHV has been detected in KS, lymphoma, and MCD, association with KSHV differs among these KSHV-associated diseases (Katano et al., 2000b; Moore and Chang, 2001). We previously revealed that almost all KS cells expressed only latent gene products, and expression of lytic proteins was rare (Katano et al., 2000b). On the other hand, various lytic proteins encoded by KSHV, e.g., vIL-6, ORF59, and K8, have been detected in MCD lesions. These observations strongly suggested that lytic replication of KSHV was crucial in pathogenesis of MCD, whereas latency of KSHV was crucial in KS cells. Results of our immunohistochemical experiments demonstrated different subcellular localizations of K10/10.1 protein between KS and MCD. This differential subcellular localization of K10/10.1 protein was also observed between unstimulated and TPA-stimulated KSHV-infected PEL cell lines. Cytoplasmic localization of K10/10.1 protein was observed only in TPA-stimulated cells. Therefore, cytoplasmic staining of K10/10.1 protein in MCD lesions suggested that B cells in the mantle zone would be in the lytic phase of KSHV infection in MCD. Other KSHV-encoded proteins such as ORF59 demonstrated different subcellular localizations between unstimulated and TPA-stimulated TY-1 or BCBL-1 as well as between KS and MCD (unpublished data). However, expression of K10/10.1 protein demonstrated a very clear difference in MCD compared with that of ORF59. Therefore, it is possible that an anti-K10 antibody will provide a useful tool for the diagnosis of KSHV-associated MCD.

PABP is a multifunctional protein and is an important molecule for mRNA stabilization, translation initiation, protection of poly(A) from nuclease activity, mRNA deadenylation, and mRNP maturation in host cells (Grosset et al., 2000; Guhaniyogi and Brewer, 2001; Minvielle-Sebastia et al., 1997). In particular, PABP may play an important role in regulating mRNA turnover by inhibiting mRNA decapping with its poly (A)-tail (Khanna and Kiledjian, 2004). PABP is predominantly present in the cytoplasm, although it is also found in the nucleus (Afonina et al., 1998). A study using GFP-tagged PABP revealed that PABP shuttled between the cytoplasm and the nucleus (Afonina et al., 1998). In the nucleus, PABP predominantly co-localizes with SC35, a splicing factor, and interacts with the poly(A)-tail (Afonina et al., 1998). It is also known that SC35 is localized close to the PML bodies in the nucleus (Maul, 1998). In the present study, immunoprecipitation suggested that a limited amount of K10/10.1 protein actually bound to PABP in KSHV-infected cells (Figs. 5C and D). IFA

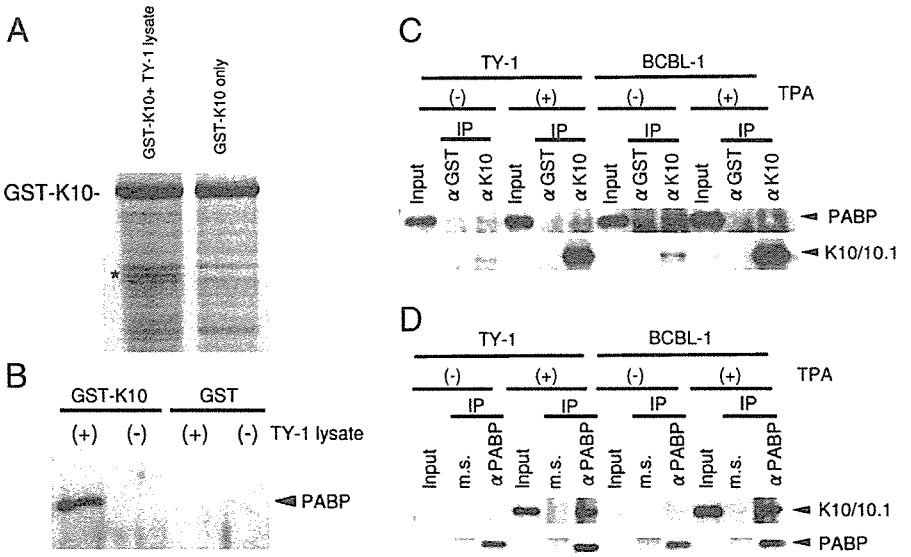

Fig. 5. K10/10.1 protein binds to PABP. (A) GST pull down assay. Ten micrograms of GST-K10 protein was incubated with TY-1 cell lysate. After adding glutathione–Sepharose beads, the beads were washed 3 times with lysis buffer. Then, the beads were loaded for SDS-PAGE using 2× sample buffer. The gel was stained with Coomassie brilliant blue. The asterisk indicates a band observed only in the lane of GST-K10 protein + TY-1 lysate, and not in the GST-K10 protein lane: as well as not in the GST protein + TY-1 lysate lane and the GST protein only lane (data not shown). (B) Western blotting of GST pulled down lysates. Beads obtained from the GST pull down assay were electrophoresed using SDS-PAGE, and blotted on a membrane. The membrane was stained with anti-PABP antibody. (C) Immunoprecipitation (IP) with anti-K10 antibody and immunoblotting with PABP. Lysates from TY-1 and BCBL-1 were immunoprecipitated with anti-K10 antibody or anti-GST antibody. Recombinant protein A-Sepharose was added and incubated. Sepharose was electrophoresed and blotted. Anti-PABP antibody was used as primary antibody for immunoblotting. Input indicates the whole lysate of TY-1 or BCBL-1 without IP. In the lower panel, anti-K10 antibody was used as primary antibody on the same membrane after stripping. (D) Immunoprecipitation with anti-PABP antibody and immunoblotting with anti-K10 antibody. Lysates from TY-1 and BCBL-1 were immunoprecipitated with anti-PABP antibody or normal mouse serum (m.s.). In the immunoblot, anti-K10 antibody was used as primary antibody for immunoblotting. In the lower panel, anti-PABP antibody was used as primary antibody on the same membrane after stripping.

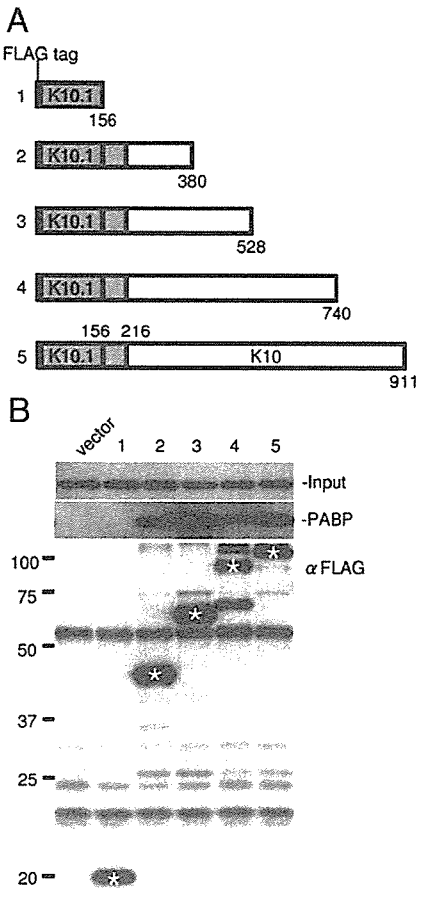

Fig. 6. Identification of the binding site of K10/10.1 protein with PABP. (A) Constructs of FLAG-tagged deletion mutants. K10/10.1 protein is composed of 911 amino acids. Four deletion mutants and a full-length K10/10.1 protein were constructed. (B) Immunoprecipitation. K10/10.1 mutants were immunoprecipitated with anti-FLAG antibody and were separated by SDS-PAGE. Endogenous PABP was detected in the top panel. Co-precipitated PABP with mutants are shown in the middle panel. Numbers on the top of the panel correspond to those in panel A. The lower panel shows sizes of deletion mutants by immunoblot using anti-FLAG antibody. Each band of mutant is indicated by white asterisks.

showed that K10/10.1 protein co-localized with PABP only in the nucleus (Fig. 7), whereas both PABP and K10/10.1 protein were present in the nucleus and cytoplasm. This might be one of the reasons why a limited amount of K10/10.1 protein bound to PABP. Overall, we can conclude that PABP forms a large complex near the PML bodies in the nucleus with SC35 and K10/10.1 protein, and is associated with mRNA turnover. It is known that some viral proteins such as poliovirus 3C protease and enterovirus proteases bind to, and cleave PABP, shutting off host translation (Joachims et al., 1999; Kuyumcu-Martinez et al., 2004). We investigated the amount of PABP in K10/10.1-transfected cells, but failed to detect changes in PABP expression levels (Kanno et al., unpublished data). Thus, K10/10.1 protein did not, at least in transfected cells, seem to directly alter PABP amount. However, our results suggested that K10/10.1 protein might inhibit function of PABP predominantly in the nucleus, resulting in shutoff of host translation. In KS cells, chemotherapy regimens including doxorubicin, bleomycin, and vincristine dramatically reduce amounts of cytoplasmic PABP, resulting in translation shutoff and G2 arrests in host cells (van der Kuyl et al., 2002). Further studies are required to clarify relationships between K10/10.1 protein and PABP.

Materials and methods

Cell culture

KSHV-harboring TY-1 cells (Katano et al., 1999b) and BCBL-1 cells (AIDS Research and Reference Reagent Program #3233, National Institutes of Health, Bethesda, MD) were cultured in RPMI 1640, in the presence of 10% FCS. HeLa and 293T cells were cultured in DMEM with 10% FCS.

Immunoscreening

A cDNA library was constructed from TPA-stimulated TY-1 cells and a KSHV-infected cell line, using *Eco*RI-predigested lambda ZAP Express vectors according to the manufacturer's instructions (Stratagene, La Jolla, CA). Immunoscreening was performed as described previously (Katano et al., 1999a). Approximately 1×10^6 phages were screened on nitrocellulose filters using an anti-K10 polyclonal antibody (Katano et al., 2000b). The antibody was diluted 1:2000 in 1 × Block Ace (Snow Brand Milk Products, Tokyo, Japan), and incubated with filters for 1 h at room temperature. Filters were washed in phosphate-buffered saline (PBS)-0.1% Tween 20, reacted with alkaline phosphatase-conjugated goat anti-rabbit immunoglobulin G (IgG, 1:5,000; Biosource), and visualized with nitroblue tetrazolium (NBT) and 5-bromo-1-chloro-3-indolylphosphate (BCIP, Promega, Madison, WI). Positive phages were selected, screened twice by the same protocol, and examined for their reactivity with the anti-K10 antibody. After conversion of positive phages into phagemids using the rapid excision system (Stratagene) and helper phages according to the manufacturer's instructions, inserts were sequenced with an ABI Prism 310 sequencer (Applied Biosystems, Foster City, CA) with the use of internal sequencing primers.

Northern blotting

Messenger RNA was extracted from TY-1 and BCBL-1 cells using a Fast Track 2.0 mRNA isolation kit (Invitrogen, Carlsbad, CA). Fifteen micrograms of mRNA were separated on 1% formaldehyde-containing agarose gel, transferred to a nylon filter, and hybridized with a probe. K10 PCR products (forward primer, 5′-CTCGGATCCCATCTACGTCCCCGTGGATA-3′; reverse primer, 5′-CTCGAATTCTGTAGATGCCGGGGATGCGC-3′; template DNA, TY-1 DNA; product size, 1767 bp) were labeled with ^{32}P (High Prime, Roche Applied Science, Mannheim, Germany), and used as probe.

Western blotting

Cell extract preparation and immunoblots were performed as described previously (Katano et al., 2001). Proteins were separated by sodium dodecyl sulfate-polyacrylamide gel electrophoresis (SDS-PAGE), probed with anti-K10 rabbit polyclonal antibody (Katano et al., 2000b) or anti-PABP mouse monoclonal antibody (ImmuQuest, Santa Cruz, CA), followed by incubation with horseradish peroxidase-conjugated anti-rabbit (or mouse) antibodies (Biosource International, Camarillo, CA), and visualization using ECL plus (Amersham Pharmacia Biotech, Buckinghamshire, UK).

Subcellular fractionation

Subcellular fractionation was prepared for TY-1 and LCL cells with/without TPA stimulation. 1×10^7 cells were lyzed in hypotonic buffer (20 mM HEPES pH 7.0, 10 mM KCl, 1 mM $MgCl_2$, 0.5 mM DTT, 0.1% Triton X-100) for 20 min on ice. After voltexing for 30 s, lysates were centrifuged at 13,000×g for 10 s. Supernatants were used as cytoplasmic fractions. Pellets were washed with hypotonic buffer twice, lyzed in extraction buffer (20% Glycerol, 420 mM NaCl, 20 mM HEPES pH 7.0, 10 mM KCl, 1 mM $MgCl_2$, 0.5 mM DTT, 0.1% Triton X-100), and centrifuged. Supernatants were used as nuclear extracts. A protease-inhibitor cocktail (Complete, EDTA-free, Roche Diagnostics, Indianapolis, IN) was added to the buffer before use.

Immunofluorescence assay (IFA)

IFA was performed as described previously (Katano et al., 2001). Anti-K10 (Katano et al., 2000b), PML (Santa Cruz Biotechnology, Santa Cruz, CA), SC35 (Sigma-Aldrich, St. Louis, MO), or PABP (ImmuQuest) antibodies were used as primary antibodies. Secondary antibodies were either Alexa-488 or Alexa-568 conjugated anti-rabbit (or anti-mouse) IgG antibodies (Molecular Probe, Eugene, OR). TOPRO3 (Molecular Probe) was used for counterstaining cell nuclei. Imaging was performed using a confocal microscope equipped with an argon–krypton laser (LSM-MicroSystem, Zeiss, Germany).

Immunohistochemistry

Formalin-fixed specimens of KS, MCD, and the animal model of KSHV-associated solid lymphoma were embedded in paraffin, sectioned, and stained with hematoxylin and eosin. Immunohistochemistry was performed with an anti-K10 rabbit polyclonal antibody (Katano et al., 2000b). For second and third phase reagents of immunostaining, a biotinylated F(ab′)2 fragment of goat anti-rabbit immunoglobulin (DAKO, Copenhagen, Denmark) and peroxidase-conjugated streptavidin (DAKO) were used. Details regarding immunostaining methods have been described previously (Katano et al., 2000b). An animal model of KSHV-associated solid lymphoma was established as described previously (Katano et al., 2000c). Briefly, TY-1 cells were inoculated into the subcutaneous tissue of mice with severe combined immunodeficiency (SCID). One month after inoculation, lymphomas appeared in the subcutaneous region at the inoculation site. Lymphoma cells contained the KSHV genome and expressed various viral proteins of KSHV (Katano et al., 2000c).

Plasmids

Expression vectors of K10/10.1 were obtained using an in vivo excision system from phage plaques (Stratagene). To construct pEGFP-K10/10.1, the K10/10.1 gene was amplified by PCR using forward (5′-CTACTCGAGCCTAAAGCC-GGTGGCTCAGAATGG-3′) and reverse (5′-CGGGGATCCT-CAATGTAGACTATCCCAAATGGA-3′) primers from the expression plasmid. PCR products were cloned into the *Xho*I/*Bam*HI sites of pEGFP (BD Biosiences Clontech, Mountain

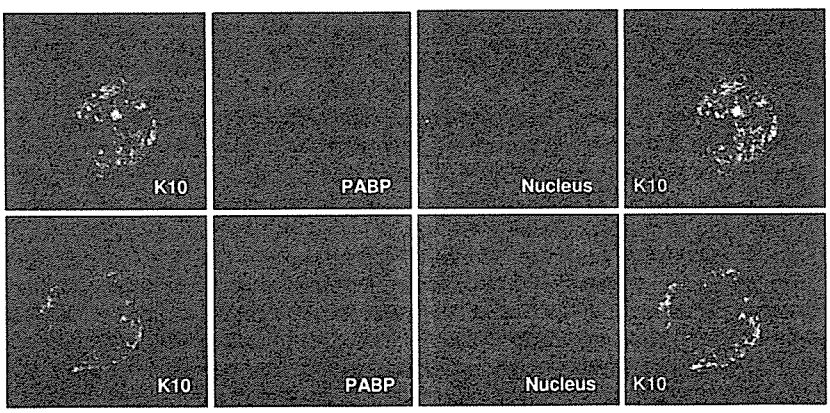

Fig. 7. IFA of TPA-stimulated TY-1 cells. K10/10.1 protein and PABP co-localize in the nucleus, but not in the cytoplasm. In some cells, K10/10.1 protein is present in the nucleus as a patchy pattern, and is diffusely distributed in the cytoplasm (upper panels). PABP co-localizes with K10/10.1 protein in the nucleus, as a patchy staining pattern in the upper panels. In the lower panels, K10/10.1 protein is expressed predominantly in the nucleus and co-localizes with PABP as a dot-like staining pattern near the nuclear membrane in the nucleus.

View, CA). For the reporter assay of interferon regulatory factors, pIFNB-Luc was constructed as reported previously (Lubyova et al., 2004). For constructions of deletion mutants, 5 fragments of K10/10.1 were amplified with PCR using one forward primer (5′-CTAGAATTCCCTAAAGCCGGTGGCTCAGAATGG-3′) and 5 reverse primers (5′-TAAGCGGCCGCTCAAACCTCACACCCCCTTC-3′ for amino acids no. 1–156, 5′-TAAGCGGCCGCTTAGAACTCACCGACAAATGTTCCCGC-3′ for amino acids no. 1–380, 5′-TAAGCGGCCGCTGGCTCCTGCGCTCTGCGACCTCT-3′ for amino acids no. 1–528, 5′-CGAGCGGCCGCTCAAAAGATTTCCACAACAAAAGACAC -3′ for amino acids no. 1–740, 5′-CATGCGGCCGCTCAATGTAGACTATCCCAAATGGA-3′ for full length of K10/10.1). PCR products were cloned into the *Eco*RI site of pME18FLAG (Ishida et al., 1996).

Transfection and luciferase assays

Expression plasmids were transfected into HeLa or 293T cells using Lipofectamine Plus (Invitrogen) for HeLa cells or Fugene 6 (Roche Diagnostics, Indianapolis, IN) for 293T cells, according to the manufacturer's instructions. An IFN promoter assay was performed as reported previously (Lubyova et al., 2004). Briefly, K10/10.1 expression plasmid and empty vector were co-transfected with pGL3-IFNB-Luc and phRL-CMV vector into HeLa cells with lipofectamine Plus (Invitrogen). Twenty-four hours after transfection, wells were washed, and Sendai virus was added to 1% BSA phosphate-buffered saline with a m.o.i of 5. Luciferase activity was measured using a dual luciferase assay system (Promega).

GST pull down assay

To identify the binding protein to K10/10.1 protein, a glutathione *S*-transferase (GST) pull down assay was performed. GST-K10 fusion gene was generated by ligation of a *Bam*HI–*Eco*RI-digested PCR product of the K10 gene to the *Bam*HI–*Eco*RI site of *p*GEX 5X-2 (Amersham Pharmacia Biotech) (Katano et al., 2000a). GST-K10 fusion protein was then expressed in *Escherichia coli*, and affinity-purified using glutathione–Sepharose as described previously (Katano et al., 2000a). Purity and concentration of eluted proteins were determined by SDS-PAGE and the Bradford assay (Protein Assay; BioRad, New York, NY), respectively. TY-1 cells (1×10^7) were washed with PBS and lyzed in 1 ml lysis buffer (50 mM Tris–HCl, pH 8.0, 150 mM NaCl, 0.1% SDS, 0.5% sodium deoxycholate, 0.5% Nonidet P-40, 1 mM phenylmethylsulfonyl fluoride, 100 U/ml aprotinin, and 0.02% sodium azide). After absorption of glutathione–Sepharose beads (Amersham Pharmacia Biotech), 10 μg GST-K10 protein or GST protein that was purified with a glutathione–Sepharose 4B column was added, and incubated at 4 °C for 2 h. Then, 25 μl glutathione–Sepharose beads were added, and incubated for 1 h. The beads were washed 3 times in carbonate buffer containing 100 mM $NaHCO_3$ and 300 mM NaCl. Bound proteins were eluted with an equal volume of 2× sampling buffer and separated by SDS-PAGE.

Mass spectrometry

Bands of interest were excised from Coomassie-stained gels, followed by destaining, reduction, alkylation, and digestion with modified porcine trypsin (Promega). Samples for MALDI-ToF analysis were prepared by mixing a small aliquot of the digested supernatant with an equal volume of a solution of alpha-cyano-4-hydroxycinnamic acid (10 mg/ml in 1:1 acetonitrile: 0.1% vol/vol trifluoroacetic acid). Peptide mass fingerprinting was performed on a reflectron MALDI-ToF mass spectrometer (Voyger, Amersham Biosciences). The Protein Prospector (http://prospector.ucsf.edu/) was employed for protein database search using monoisotopic mass values for each spectrum.

Immunoprecipitation

Cells (1×10^6) were lyzed in 1 ml lysis buffer (50 mM Tris–HCl, pH 8.0, 150 mM NaCl, 1% Nonidet P-40, 1 mM phenylmethylsulfonyl fluoride, 100 U/ml aprotinin, 1 mM DTT). After absorption of recombinant protein A–Sepharose (Amersham Pharmacia Biotech, Buckinghamshire, UK), equal amounts of cell lysates were incubated with equal amounts of a polyclonal antibody against the K10 protein or preimmune-rabbit serum. The proteins separated by SDS-PAGE were transferred onto membranes (Immobilon; Millipore, Bedford, MA).

Deletion mutants

Plasmids expressing mutant K10/10.1 were transfected in 293T cells. Transfectants were lyzed, and equal amounts of lysate were incubated with anti-FLAG M2 antibody (Sigma). Recombinant protein A-Sepharose was added, and proteins were separated by SDS-PAGE. Endogenous PABP was detected on a blotted membrane using anti-PABP antibody.

Acknowledgments

The authors would like to thank Dr. Atsushi Kato of the Department of Virology 3 at the National Institute of Infectious Diseases for providing Sendai virus samples, and Drs. Fumiko Shinkai-Ouchi and Yoshio Yamakawa of the Department of Biochemistry and Cell Biology at the National Institute of Infectious Diseases for their technical assistance on mass spectrometry. This research was supported by Health and Labor Sciences Research Grants on HIV/AIDS and Measures for Intractable Diseases from the Ministry of Health, Labor and Welfare (grants H15-AIDS-005 to H.K., and 17243601 to T.S.), a Grants-in-Aid for Scientific Research from the Ministry of Education, Culture, Sports, Science and Technology of Japan (grant 17590365 to H.K.), and a grant for Research on Health Sciences focusing on Drug Innovation from Japan Health Sciences Foundation (grant SA14831 to H.K).

References

Afonina, E., Stauber, R., Pavlakis, G.N., 1998. The human poly(A)-binding protein 1 shuttles between the nucleus and the cytoplasm. J. Biol. Chem. 273, 13015–13021.

Burysek, L., Pitha, P.M., 2001. Latently expressed human herpesvirus 8-encoded interferon regulatory factor 2 inhibits double-stranded RNA-activated protein kinase. J. Virol. 75, 2345–2352.

Burysek, L., Yeow, W.S., Lubyova, B., Kellum, M., Schafer, S.L., Huang, Y.Q., Pitha, P.M., 1999. Functional analysis of human herpesvirus 8-encoded viral interferon regulatory factor 1 and its association with cellular interferon regulatory factors and p300. J. Virol. 73, 7334–7342.

Cunningham, C., Barnard, S., Blackbourn, D.J., Davison, A.J., 2003. Transcription mapping of human herpesvirus 8 genes encoding viral interferon regulatory factors. J. Gen. Virol. 84, 1471–1483.

Fakhari, F.D., Dittmer, D.P., 2002. Charting latency transcripts in Kaposi's sarcoma-associated herpesvirus by whole-genome real-time quantitative PCR. J. Virol. 76, 6213–6223.

Grosset, C., Chen, C.Y., Xu, N., Sonenberg, N., Jacquemin-Sablon, H., Shyu, A.B., 2000. A mechanism for translationally coupled mRNA turnover: interaction between the poly(A) tail and a c-*fos* RNA coding determinant via a protein complex. Cell 103, 29–40.

Guhaniyogi, J., Brewer, G., 2001. Regulation of mRNA stability in mammalian cells. Gene 265, 11–23.

Ishida, T.K., Tojo, T., Aoki, T., Kobayashi, N., Ohishi, T., Watanabe, T., Yamamoto, T., Inoue, J., 1996. TRAF5, a novel tumor necrosis factor receptor-associated factor family protein, mediates CD40 signaling. Proc. Natl. Acad. Sci. U.S.A. 93, 9437–9442.

Jenner, R.G., Alba, M.M., Boshoff, C., Kellam, P., 2001. Kaposi's sarcoma-associated herpesvirus latent and lytic gene expression as revealed by DNA arrays. J. Virol. 75, 891–902.

Joachims, M., Van Breugel, P.C., Lloyd, R.E., 1999. Cleavage of poly(A)-binding protein by enterovirus proteases concurrent with inhibition of translation in vitro. J. Virol. 73, 718–727.

Katano, H., Hoshino, Y., Morishita, Y., Nakamura, T., Satoh, H., Iwamoto, A., Herndier, B., Mori, S., 1999a. Establishing and characterizing a CD30-positive cell line harboring HHV-8 from a primary effusion lymphoma. J. Med. Virol. 58, 394–401.

Katano, H., Sata, T., Suda, T., Nakamura, T., Tachikawa, N., Nishizumi, H., Sakurada, S., Hayashi, Y., Koike, M., Iwamoto, A., Kurata, T., Mori, S., 1999b. Expression and antigenicity of human herpesvirus 8 encoded ORF59 protein in AIDS-associated Kaposi's sarcoma. J. Med. Virol. 59, 346–355.

Katano, H., Iwasaki, T., Baba, N., Terai, M., Mori, S., Iwamoto, A., Kurata, T., Sata, T., 2000a. Identification of antigenic proteins encoded by human herpesvirus 8 and seroprevalence in the general population and among patients with and without Kaposi's sarcoma. J. Virol. 74, 3478–3485.

Katano, H., Sato, Y., Kurata, T., Mori, S., Sata, T., 2000b. Expression and localization of human herpesvirus 8-encoded proteins in primary effusion lymphoma, Kaposi's sarcoma, and multicentric Castleman's disease. Virology 269, 335–344.

Katano, H., Suda, T., Morishita, Y., Yamamoto, K., Hoshino, Y., Nakamura, K., Tachikawa, N., Sata, T., Hamaguchi, H., Iwamoto, A., Mori, S., 2000c. Human herpesvirus 8-associated solid lymphomas that occur in AIDS patients take anaplastic large cell morphology. Mod. Pathol. 13, 77–85.

Katano, H., Ogawa-Goto, K., Hasegawa, H., Kurata, T., Sata, T., 2001. Human-herpesvirus-8-encoded K8 protein colocalizes with the promyelocytic leukemia protein (PML) bodies and recruits p53 to the PML bodies. Virology 286, 446–455.

Khanna, R., Kiledjian, M., 2004. Poly(A)-binding-protein-mediated regulation of hDcp2 decapping in vitro. EMBO J. 23, 1968–1976.

Kuyumcu-Martinez, N.M., Van Eden, M.E., Younan, P., Lloyd, R.E., 2004. Cleavage of poly(A)-binding protein by poliovirus 3C protease inhibits host cell translation: a novel mechanism for host translation shutoff. Mol. Cell. Biol. 24, 1779–1790.

Li, M., Lee, H., Guo, J., Neipel, F., Fleckenstein, B., Ozato, K., Jung, J.U., 1998. Kaposi's sarcoma-associated herpesvirus viral interferon regulatory factor. J. Virol. 72, 5433–5440.

Lubyova, B., Pitha, P.M., 2000. Characterization of a novel human herpesvirus 8-encoded protein, vIRF-3, that shows homology to viral and cellular interferon regulatory factors. J. Virol. 74, 8194–8201.

Lubyova, B., Kellum, M.J., Frisancho, A.J., Pitha, P.M., 2004. Kaposi's sarcoma-associated herpesvirus-encoded vIRF-3 stimulates the transcriptional activity of cellular IRF-3 and IRF-7. J. Biol. Chem. 279, 7643–7654.

Maul, G.G., 1998. Nuclear domain 10, the site of DNA virus transcription and replication. BioEssays 20, 660–667.

Minvielle-Sebastia, L., Preker, P.J., Wiederkehr, T., Strahm, Y., Keller, W., 1997. The major yeast poly(A)-binding protein is associated with cleavage factor IA and functions in premessenger RNA 3′-end formation. Proc. Natl. Acad. Sci. U.S.A. 94, 7897–7902.

Moore, P.S., Chang, Y., 2001. In: Knipe, D.M., Howley, P.M. (Eds.), Kaposi's Sarcoma-Associated Herpesvirus, 4th ed. Lippincott Williams and Wilkins, Philadelphia.

Pozharskaya, V.P., Weakland, L.L., Zimring, J.C., Krug, L.T., Unger, E.R., Neisch, A., Joshi, H., Inoue, N., Offermann, M.K., 2004. Short duration of elevated vIRF-1 expression during lytic replication of human herpesvirus 8 limits its ability to block antiviral responses induced by alpha interferon in BCBL-1 cells. J. Virol. 78, 6621–6635.

Rivas, C., Thlick, A.E., Parravicini, C., Moore, P.S., Chang, Y., 2001. Kaposi's sarcoma-associated herpesvirus LANA2 is a B-cell-specific latent viral protein that inhibits p53. J. Virol. 75, 429–438.

Sun, R., Lin, S.F., Staskus, K., Gradoville, L., Grogan, E., Haase, A., Miller, G., 1999. Kinetics of Kaposi's sarcoma-associated herpesvirus gene expression. J. Virol. 73, 2232–2242.

van der Kuyl, A.C., van den Burg, R., Zorgdrager, F., Dekker, J.T., Maas, J., van Noesel, C.J., Goudsmit, J., Cornelissen, M., 2002. Primary effect of chemotherapy on the transcription profile of AIDS-related Kaposi's sarcoma. BMC Cancer 2, 21.

Zimring, J.C., Goodbourn, S., Offermann, M.K., 1998. Human herpesvirus 8 encodes an interferon regulatory factor (IRF) homolog that represses IRF-1-mediated transcription. J. Virol. 72, 701–707.

Jpn J Ophthalmol 2006;50:7–11
© Japanese Ophthalmological Society 2006
DOI 10.1007/s10384-005-0268-y

LABORATORY INVESTIGATION

Human Herpesvirus-8 in Kaposi's Sarcoma of the Conjunctiva in a Patient with AIDS

Hiroshi Minoda[1], Norio Usui[2], Tetsutaro Sata[3], Harutaka Katano[3], Hiromi Serizawa[4], and Shinya Okada[4]

[1]Department of Ophthalmology, Tokyo Medical University, Tokyo, Japan; [2]Shinkawabashi Hospital, Kawasaki, Japan; [3]Department of Pathology, National Institute of Infectious Diseases, Tokyo, Japan; [4]Department of Pathology, Tokyo Medical University, Tokyo, Japan

Abstract

Purpose: To demonstrate human herpesvirus-8 (HHV-8) in Kaposi's sarcoma (KS) of the conjunctiva in a patient with acquired immunodeficiency syndrome (AIDS).

Methods: Clinical observation, pathologic findings of conjunctival specimens, immunohistochemical staining for HHV-8-specific antigen, polymerase chain reaction (PCR) analysis of HHV-8 DNA, and detection of specific antibody in patient's serum at appropriate times.

Results: In the conjunctival specimen, swollen endothelial-like cells were found with slit-like vessels. CD 31-positive cells were noted on the inner surface of the slit-like vessels, and HHV-8 latency-associated nuclear antigen was detected. The presence of HHV-8 DNA was demonstrated by PCR. Anti-HHV-8 antibody was found in the patient's serum.

Conclusions: This is the first case report in the ophthalmology literature that provides histological, DNA, and serological evidence that HHV-8 is involved in the pathogenesis of conjunctival KS. **Jpn J Ophthalmol** 2006;50:7–11 © Japanese Ophthalmological Society 2006

Key Words: AIDS, conjunctiva, human herpesvirus-8, Kaposi's sarcoma, latency-associated nuclear antigen

Introduction

Kaposi's sarcoma (KS) is a malignant vascular neoplasm originally reported as a local disease in elderly people of Mediterranean countries. With the increase in acquired immunodeficiency syndrome (AIDS) cases, KS has been reported to be the most frequent malignant tumor developing in AIDS patients, especially among homosexual men in the United States. In the early 1980s, 15%–20% of AIDS patients developed KS,[1] and one-third of the patients were homosexual.[2] About 2% of AIDS patients developed KS either in the eyelids or conjunctiva,[3] but such cases are extremely rare and no documentation is available.

In 1994, specific herpesvirus-like DNA sequences were found in KS lesions of an AIDS patient, suggesting that a novel gamma herpesvirus, homologous to Epstein-Barr virus, exists in KS.[4] Subsequently, the virus was named human herpesvirus-8 (HHV-8). Thereafter, a number of viral studies have been performed on KS. However, there is no report in the field of ophthalmology that provides direct evidence of the involvement of HHV-8 in ocular lesions. In this study, we examined and treated an AIDS patient with ocular KS and detected HHV-8-specific antigen and HHV-8 DNA in conjunctival tissue as well as HHV-8-specific antibody in the serum. We present the clinical findings of this case because ocular KS is very rare in Japan. This case report also provides direct evidence for the first time in the

Received: January 18, 2005 / Accepted: April 26, 2005
Correspondence and reprint requests to: Hiroshi Minoda, Department of Ophthalmology, Tokyo Medical University, 6-7-1 Nishishinjuku, Shinjuku-ku, Tokyo 160-0023, Japan
e-mail: damino@za.pial.jp

Jpn J Ophthalmol
Vol 50: 7–11, 2006

ophthalmological literature that HHV-8 is involved in ocular KS.

Case Presentation

A 33-year-old homosexual Japanese man visited a dentist on June 19, 1999 because of swelling of the gingiva since early June (Fig. 1). A blood test was positive for human immunodeficiency virus (HIV) antibody. He was hospitalized in Tokyo Medical University Hospital, owing to fever and dyspnea, on June 26. AIDS was diagnosed based on a decreased CD4+ cell count (4/μl) and remarkably lowered cell-mediated immunity. After admission, a dark purple eruption was recognized on his trunk in addition to the gingival lesion. On June 30, he complained of feeling foreign bodies in both eyes and pain in the right eye, and underwent ophthalmological examinations. Two dark red, flatly elevated lesions 4 mm in width were recognized on the conjunctiva of both lower lids, and pedunculate lesions 3–4 mm in width were observed in the whole lower part of the conjunctival fornix and the medial canthus. Partial hemorrhage was observed in these lesions (Fig. 2). Abrasion by the lesion while blinking was considered to have produced epithelial erosion of the cornea. No abnormal findings were observed in the medial or posterior segments of the eyes. Bilateral pleural effusion and infiltration in the right and left lower lung fields were recognized by both chest X-ray and computed tomography (CT) examination.

Pathological examinations of the gingival lesions and transbronchial-lung biopsy specimens revealed proliferation of spindle cells and some specimens with vascular cavities, and KS was diagnosed. Highly active antiretroviral therapy using sanilvudine, lamivudine, and indinavir was started on July 8 as an anti-HIV treatment. Systemic administration of foscavir (120 mg/kg per day) for KS was given simultaneously for 21 days, from July 9 to July 29, but no tumor reduction was recognized. Invasion of the sarcoma from the mouth into the larynx increased the risk of airway obstruction, and the remarkable growth of sarcoma in the lungs, skin, and eyelids necessitated administration of doxorubicin hydrochloride (20 mg/m^2), bleomycin hydrochloride (20 mg/m^2), and vincristine sulfate (2 mg/m^2) from July 28.

After the chemotherapy, gum swelling and eruption on the trunk were reduced, and regression of sarcoma in the lung was confirmed by chest X-ray and CT. Although sarcoma of the eyelid showed some reduction in size, on August 6 we surgically removed a lesion at the lower eyelid fornix with microscissors under local anesthesia, for the purpose of definitive diagnosis and treatment evaluation. Pathological examination and molecular biological study for HHV-8 were performed on the specimen. In addition, we collected serum during the episode to examine anti-HHV-8 antibody. No recurrence of sarcoma was observed in the eyelids until January 2005, but eruption on the trunk and sarcoma in other locations recurred repeatedly, and regressed after reuse of chemotherapy. However, the number of CD-4-positive cells has increased, and no recurrence of the eruptions has been observed since August 2001.

Materials and Methods

This study was approved by the Ethics Committee of Tokyo Medical University.

Histopathology

The surgically removed specimen (18 mm × 2 mm) was fixed in 10% formalin, and the paraffin sections were stained with hematoxylin and eosin (H&E).

Immunohistochemistry

The deparaffinized sections were immunostained by the labeled streptavidin–biotin method (Dako, Glostrup, Denmark) using anti-human CD 31 mouse monoclonal antibody for vascular endothelial cells (Dako).[5]

To identify HHV-8 in the tumor tissue, we used a rabbit antibody (PA1-73N)[6] to ORF 73 protein, which is a latency-associated nuclear antigen (LANA) expressed in the latent phase of HHV-8 infection. The 4-μm sections were deparaffinized by sequential immersion in xylene and ethanol, rehydrated in distilled water, and irradiated for 15 min in a microwave oven for antigen retrieval. Endogenous peroxidase activity was blocked by immersing the sections in a methanol/0.6% H_2O_2 solution for 30 min at room temperature. Affinity-purified PA1-73N antibody [diluted 1:3000 in phosphate-buffered saline (PBS)/5% bovine serum albumin] was then applied, and the sections were incubated overnight at 4°C. After washing in PBS twice, the second and third reactions and the amplification procedure were performed using a kit (Dako) according to the manufacturer's instructions. The signals were visualized using 0.2 mg/ml diaminobenzidine and 0.015% H_2O_2 in 0.05 mol/l Tris-HCl, pH 7.6. Double immunostaining for LANA was performed as described previously.[7]

DNA Isolation by Polymerase Chain Reaction

Polymerase chain reaction (PCR) analysis for HHV-8 DNA was performed on conjunctival tissues. An HHV-8 DNA-positive cell line (TY-1)[8] established from an HHV-8-related tumor (primary effusion lymphoma) found in an AIDS patient was used as positive control. An HHV-8 DNA-negative cell line established from human umbilical vascular endothelial cells (HUVEC) was used as negative control. Total DNA was extracted by proteinase K digestion and phenol–chloroform–isoamyl alcohol treatment, as used routinely. PCR for HHV-8 DNA using KSBam$_{330}$233 was performed as described previously.[4] The PCR products were electrophoresed in 2% agarose gels to identify the 233-bp

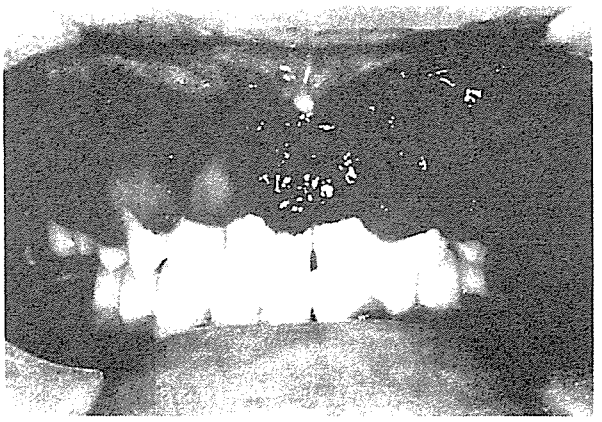

Figure 1. Buccal cavity. The entire maxillary buccal gingival area is swollen, and dark red tumors are observed in a patient with acquired immunodeficiency syndrome (AIDS) and Kaposi's sarcoma (KS).

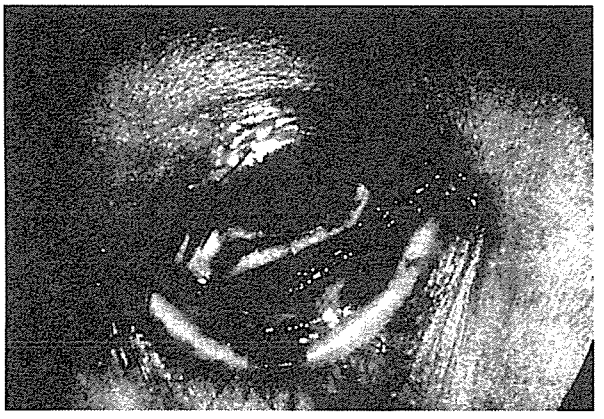

Figure 2. The right eye. Two dark red, flatly elevated lesions are recognized in the lower lid conjunctiva, and pedunculate lesions are observed in the entire lower conjunctival fornix and medial canthus. Partial hemorrhage is visible.

fragment and visualized by ethidium bromide staining under ultraviolet transillumination.

Serology

An immunofluorescence assay (IFA) was carried out as described previously.[9,10] To detect anti-HHV-8 serum antibodies, we first propagated TY-1 cells by adding 20 ng/ml tetradecanoyl phorbol ester (TPA) to the culture medium for 48 h. After washing twice in PBS, the TPA-induced TY-1 cells were spotted onto a slide (Erie Scientific, Erie, CO, USA), dried, and then fixed in acetone for 10 min at room temperature. The patient's serum was diluted 1:40 in PBS–2% fetal calf serum and applied to the slide for 45 min at room temperature. Rabbit anti-human IgG conjugated

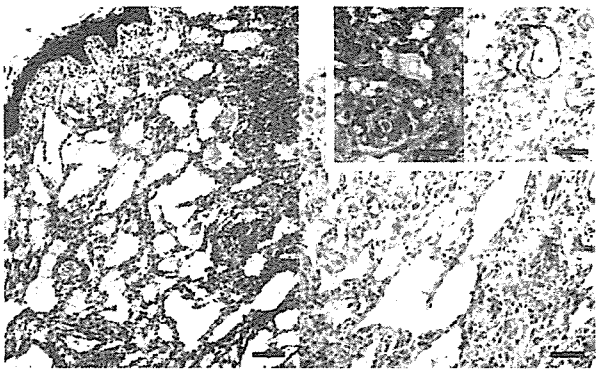

Figure 3. Conjunctival sample. Histopathological findings (H&E staining, *left*) show spindle-shaped cell proliferation and multiple slit-like vessels. A typical swollen endothelial cell is found in the lumen of the slit-like vessels. Among the vessels, spindle-shaped tumor cells are distributed, some showing a fascicular pattern. Bar = 200 μm. Immunohistochemical staining (anti-CD 31, ×40, *right*) shows CD 31-positive cells on the inner surface of the slit-like vessels. Bar = 400 μm. Inset: Bar = 800 μm.

with fluorescein isothiocyanate (Tago Immunologicals, Camarillo, CA, USA) was used as the secondary antibody. Between these steps, the slides were washed three times each in PBS for 5 min. A positive reaction of HHV-8 antibody by IFA was determined by the presence of LANA, other nuclear antigens, and/or cytoplasmic antigens.

Results

Pathology

Tumors were located just below the conjunctival epithelium. Histopathologically, proliferation of spindle-shaped cells and multiple slit-like vessels were observed. Typical swollen endothelial cells lined the lumen of the slit-like vessels. Among these vessels, spindle-shaped tumor cells were distributed, and some of them showed a fascicular pattern (Fig. 3).

Immunohistochemistry

CD 31-positive cells were noted on the inner surface of the slit-like vessels, indicating that the cells forming the slit-like structures were of vascular endothelial cell origin (Fig. 3). Using anti-LANA antibody, dot-shaped staining reactions were observed in the nuclei of the spindle-shaped cells, indicating the presence of the ORF73 protein of HHV-8 in these cells (Fig. 4).

Polymerase Chain Reaction

Agarose gel electrophoresis of the PCR products showed human β-globin DNA (248 bp) in all samples, confirming the

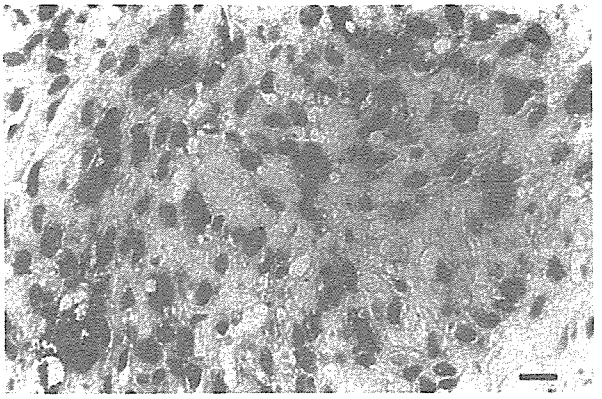

Figure 4. Immunohistochemical staining (anti-latency-associated nuclear antigen, anti-LANA) of the conjunctival sample. Dot-shaped staining reactions are observed in the nuclei of the spindle-shaped cells. Bar = 10μm.

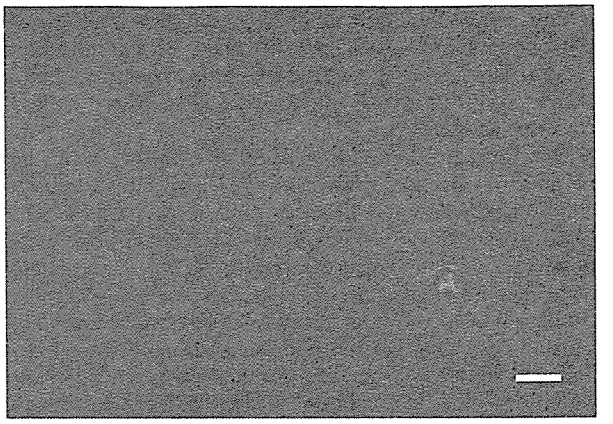

Figure 6. Serum anti-HHV-8 antibodies are detected by an indirect immunofluorescence method using acetone-fixed TY-1 cells, showing mainly LANA in the nuclei. Bar = 10μm.

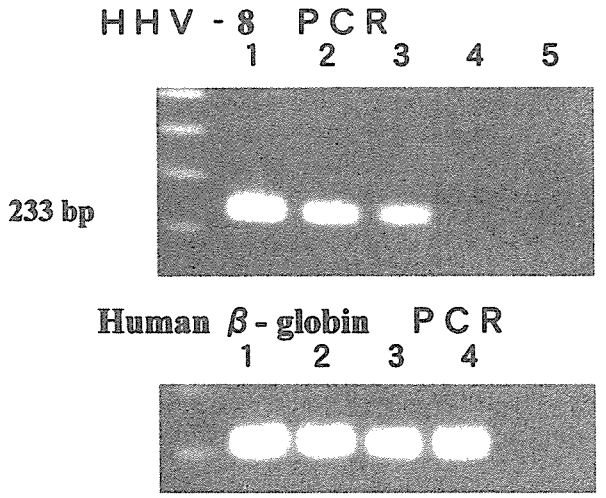

Figure 5. Polymerase chain reaction (*PCR*) analysis using patient's conjunctival KS sample. *Lane 1*, TY-1 cell [human herpesvirus (*HHV*)-8 positive]; *lane 2*, patient's sample 1; *lane 3*, patient's sample 2; *lane 4*, HUVEC (HHV-8 negative); *lane 5*, double sterilized water (negative control). The 233-bp target sequence of HHV-8 is detected in the conjunctival KS tumor and TY-1 cells. *Human β-globin* DNA (248bp) is demonstrated in all samples, confirming the quality of DNA samples.

quality of the DNA samples. The 233-bp target sequence of HHV-8 was detected in the conjunctival KS tumor and in the TY-1 cells (Fig. 5).

Serology

Anti-HHV-8 antibody was detected in the serum, and the antibody titer was estimated to be 1:40 (Fig. 6).

Discussion

Kaposi's sarcoma is the most common neoplasm in patients infected with HIV. Prior to the AIDS epidemic, this tumor was exceedingly rare, but it is now very common, particularly in patients with AIDS. The incidence in homosexual men with AIDS is 20 times that in hemophilic patients,[11] but the pathogenesis of AIDS-related KS is unknown. KS usually occurs when CD4-positive cells decrease to less than 200/μl, but KS has also been reported in a patient with more than 500/μl of CD4.[12] When associated with AIDS, KS is particularly aggressive, affecting mainly the skin and disseminating to visceral organs such as the gastrointestinal tract, lung, and liver. AIDS-associated ocular KS usually occurs in the eyelids or conjunctiva in the late course of the disease. The lesion may be flat or raised at the lower fornix and is bright red and surrounded by tortuous, dilated vessels, resembling subconjunctival hemorrhage. Clinically, ocular KS is classified into three stages.[13] In stages 1 and 2, the tumors are patchy and flat (less than 3mm high) and in stage 3, the tumors are nodular and elevated (more than 3 mm high).

Histologically, stage 1 lesions consist of thin-walled, dilated vascular channels lined with flat endothelial cells, and they are often filled with erythrocytes. Mitotic figures are not usually seen. Features of stage 2 lesions are plump, fusiform cells that form thin-walled, dilated, and empty vascular channels. A number of these cells have hyperchromatic nuclei. Stage 3 lesions are characterized by large aggregates of densely packed spindle cells with slit-like spaces, many of which contain erythrocytes. The lesion of our patient was classified as stage 3, both clinically and histologically.

The treatment of ocular KS depends on the ocular symptoms as well as on the general condition of the patient. If the patient has no ocular symptoms, no local treatment is

required. Surgery is a safer and more effective treatment option, depending on the clinical and histopathological stage of the tumor and its location. Stage 3 KS of the bulbar conjunctiva should be excised surgically, preferably under better visualization of the tumor-associated vessels by fluorescein angiography.

We detected DNA fragments of HHV-8 from the resected conjunctival tissue. In 1994, Chang et al.[4] reported two DNA fragments of 330bp and 631bp, which were detected specifically in the KS lesion of AIDS patients by representational difference analysis (RDA). They named them Kaposi's sarcoma-associated herpesvirus-like DNA, owing to DNA homology with herpesvirus saimiri and Epstein-Barr virus. However, the agent has now been determined to be HHV-8, since not only DNA fragments but also whole infective virus have been found in the lesion. Recently, HHV-8 DNA has been identified in KS lesions of various organs such as skin, gastrointestinal tract,[4] lymph node,[14] lung, liver, pericardium, prostate gland,[15] oral mucosa,[16] pancreas, and intestinal tract.[17] However, HHV-8 DNA has not been reported heretofore in an ocular KS lesion.

ORF73 protein antigen is known to appear in the nuclei of cells latently infected by HHV-8. Therefore, the fact that most of the spindle cells, the main component of KS, are positive for ORF73 suggests that HHV-8 exists in a latent state in KS.[6] Our immunohistological examination supported this conclusion, that HHV-8 should be identified as a possible cause of ocular KS.

Serological examination also suggested that HHV-8 was responsible for KS in our patient. The infection route and pathology of HHV-8 are still obscure, but HHV-8 may be sexually transmitted. A previous report showed that anti-HHV-8 serum antibody was positive in 88% of an AIDS-associated KS group, in 30% of an HIV-positive (without KS) group, and in 1%–4% of a normal group.[18] Additionally, the antibody titer of the sexually transmitted HIV group was markedly higher than that of the HIV group with other routes of infection.[19] It has also been reported that the appearance of anti-HHV-8 antibody precedes the onset of KS.[20] Our patient was also a homosexual man without a history of transfusion or surgery, and he was serologically positive for HHV-8. Recently, ORF73 has been observed in conjunctival KS.[21] Our detailed analyses of the present case further provide histological, DNA and serological evidence more directly linking HHV-8 to the pathogenesis of conjunctival KS. Since ocular KS is still rarely encountered in Japan, our comprehensive coverage of ocular and systemic lesions may provide ophthalmologists and general physicians with a more complete clinical profile of KS in AIDS patients. KS is a treatable disease if diagnosed promptly. However, specific treatment for KS has not yet been established. New effective agents that not only promote regression of KS lesions but also prevent recurrence are needed at present.

Acknowledgments. The authors appreciate the helpful suggestions by Dr. M. Usui. We also thank Dr. K. Fukutake for editorial assistance.

References

1. Beral V, Peterman TA, Berkelman RL, Jaffe HW. Kaposi's sarcoma among persons with AIDS: a sexually transmitted infection? Lancet 1990;335:123–128.
2. Havercos HW, Drotman DP. Prevalence of Kaposi's sarcoma among patients with AIDS. N Engl J Med 1985;312:1518.
3. Jabs DA, Quinn TC. Acquired immunodeficiency syndrome. In: Pepose JS, Holland GN, Wilhelmus KR, editors. Ocular Infection and Immunity. St. Louis: Mosby, 1996: p. 289–310.
4. Chang Y, Cesarman E, Pessin MS, et al. Identification of herpesvirus-like DNA sequences in AIDS-associated Kaposi's sarcoma. Science 1994;266:1865–1869.
5. Parums DV, Cordell JL, Micklem K, et al. JC70: a new monoclonal antibody that detects vascular endothelium associated antigen on routinely processed tissue sections. J Clin Pathol 1990;43:752–757.
6. Katano H, Sato Y, Kurata T, et al. High expression of HHV-8-encoded ORF73 protein in spindle-shaped cells of Kaposi's sarcoma. Am J Pathol 1999;155:47–52.
7. Katano H, Morishita Y, Cui LX, et al. Expression of latent membrane protein 1 in clinically isolated cases and animal models of AIDS-associated non-Hodgkin's lymphomas. Pathol Int 1996;46:568–574.
8. Katano H, Hoshino Y, Morishita Y, et al. Establishing and characterizing a CD30-positive cell line harboring HHV-8 from a primary effusion lymphoma. J Med Virol 1999;58:394–401.
9. Kedes DH, Ganem D, Ameli N, et al. The prevalence of serum antibody to human herpesvirus 8 (Kaposi's sarcoma-associated herpesvirus) among HIV-seropositive and high risk HIV seronegative women. JAMA 1997;277:478–481.
10. Simpson GR, Schulz TF, Whitby D, et al. Prevalence of Kaposi's sarcoma associated herpesvirus infection measured by antibodies to recombinant capsid protein and latent immunofluorescence antigen. Lancet 1996;348:1133–1138.
11. Beral V, Bull D, Darby S, et al. Risk of Kaposi's sarcoma and sexual practices associated with faecal contact in homosexual or bisexual men with AIDS. Lancet 1992;339:632–635.
12. Orfanos CE, Husak R, Wölfer U, et al. Kaposi's sarcoma: a reevaluation. Recent Results Cancer Res 1995;139:275–296.
13. Dugel PU, Gill PS, Frangieh GT, et al. Ocular adnexal Kaposi's sarcoma in acquired immunodeficiency syndrome. Am J Ophthalmol 1990;110:500–503.
14. Su I, Hsu Y, Chang Y, et al. Herpesvirus-like DNA sequence in Kaposi's sarcoma from AIDS and non-AIDS patients in Taiwan. Lancet 1995;345:722–723.
15. Corbellino M, Poirel L, Bestetti G, et al. Restricted tissue distribution of extralesional Kaposi's sarcoma-associated herpesvirus-like DNA sequences in AIDS patients with Kaposi's sarcoma. AIDS Res Hum Retroviruses 1996;12:651–657.
16. Webster-Cyriaque J, Edwards RH, Quinlivan EB, et al. Epstein-Barr virus and human herpesvirus 8 prevalence in human immunodeficiency virus associated oral mucosal lesions. J Infect Dis 1997;175:1324–1332.
17. Cathomas G, Stalder A, McGandy CE, et al. Distribution of human herpesvirus 8 DNA in tumorous and nontumorous tissue of patients with acquired immunodeficiency syndrome with and without Kaposi's sarcoma. Mod Pathol 1998;11:415–420.
18. Gao SJ, Kingsley L, Li M, et al. KSHV antibodies among Americans, Italians and Ugandans with and without Kaposi's sarcoma. Nat Med 1996;2:925–928.
19. Kedes DH, Operskalski E, Busch M, et al. The seroepidemiology of human herpesvirus 8 (Kaposi's sarcoma-associated herpesvirus): distribution of infection in KS risk groups and evidence for sexual transmission. Nat Med 1996;2:918–924.
20. Gao SJ, Kingsley L, Hoover DR, et al. Seroconversion to antibodies against Kaposi's sarcoma-associated herpesvirus-related latent nuclear antigens before the development of Kaposi's sarcoma. N Engl J Med 1996;335:233–241.
21. Hasche H, Eck M, Lieb W. Immunochemical demonstration of human herpesvirus 8 in conjunctival Kaposi's sarcoma [in German]. Ophthalmologe 2003;100:142–144.

Journal of Pathology
J Pathol 2006; **209**: 464–473
Published online 1 June 2006 in Wiley InterScience
(www.interscience.wiley.com) **DOI:** 10.1002/path.2012

Original Paper

Effusion and solid lymphomas have distinctive gene and protein expression profiles in an animal model of primary effusion lymphoma

Y Yanagisawa,[1] Y Sato,[2] Y Asahi-Ozaki,[2] E Ito,[1] R Honma,[1] J Imai,[1] T Kanno,[2] M Kano,[2] H Akiyama,[2] T Sata,[2] F Shinkai-Ouchi,[3] Y Yamakawa,[3] S Watanabe[1] and H Katano[2]*

[1]*Department of Clinical Informatics, Tokyo Medical and Dental University, Tokyo, Japan*
[2]*Department of Pathology, National Institute of Infectious Diseases, Tokyo, Japan*
[3]*Department of Biochemistry and Cell Biology, National Institute of Infectious Diseases, Tokyo, Japan*

*Correspondence to:
Dr H Katano, Department of Pathology, National Institute of Infectious Diseases, 1-23-1 Toyama, Shinjuku, Tokyo 162-8640, Japan.
E-mail: katano@nih.go.jp

Received: 26 December 2005
Revised: 7 March 2006
Accepted: 17 April 2006

Abstract

Lymphoma usually forms solid tumours in patients, and high expression levels of adhesion molecules are observed in these tumours. However, Kaposi's sarcoma-associated herpesvirus (KSHV)-related primary effusion lymphoma (PEL) does not form solid tumours and adhesion molecule expression is suppressed in the cells. Inoculation of a KSHV-associated PEL cell line into the peritoneal cavity of severe combined immunodeficiency mice resulted in the formation of effusion and solid lymphomas in the peritoneal cavity. Proteomics using two-dimensional difference gel electrophoresis and DNA microarray analyses identified 14 proteins and 105 genes, respectively, whose expression differed significantly between effusion and solid lymphomas. Five genes were identified as having similar expression profiles to that of lymphocyte function-associated antigen 1, an important adhesion molecule in leukocytes. Among these, coronin 1A, an actin-binding protein, was identified as a molecule showing high expression in solid lymphoma by both DNA microarray and proteomics analyses. Western and northern blotting showed that coronin 1A was predominantly expressed in solid lymphomas. Moreover, KSHV-encoded lytic proteins, including viral interleukin-6, were highly expressed in effusion lymphoma compared with solid lymphoma. These data demonstrate that effusion and solid lymphomas possess distinctive gene and protein expression profiles in our mouse model, and suggest that differences in gene and protein expression between effusion and solid lymphomas may be associated with the formation of effusion lymphoma or invasive features of solid lymphoma. Furthermore, the results obtained using this combination of proteomics and DNA microarray analyses indicate that protein synthesis partly reflects, but does not correlate strictly with, mRNA production.

Keywords: primary effusion lymphoma; animal model; proteomics; DNA microarray; Kaposi's sarcoma-associated herpesvirus

Introduction

Primary effusion lymphoma (PEL), also known as body cavity-based lymphoma (BCBL), is a rare complication in patients with acquired immunodeficiency syndrome (AIDS) [1–4], and has a unique character compared with other types of lymphoma. While all other types of lymphoma form solid tumours in lymph nodes or extranodal sites, PEL cells proliferate in the peritoneal, abdominal or pericardial cavity of patients as lymphomatous effusions [2]. Curiously, PEL rarely progresses to leukaemia, and PEL cells prefer to grow as effusions in these body cavities [2]. PEL is known to be associated with Kaposi's sarcoma-associated herpesvirus (KSHV, human herpesvirus 8) infection [1,2,4]. KSHV-encoded latency-associated nuclear antigen (LANA, ORF73) is detected in the nucleus of almost all PEL cells, suggesting that KSHV infects PEL cells in the latent phase [5–7]. KSHV infection is also associated with a type of solid lymphoma (KSHV-associated solid lymphoma) [5,8], which occurs in the skin, lungs and gastrointestinal tract of AIDS patients with homosexual behaviour and sometimes complicates other KSHV-associated diseases, such as Kaposi's sarcoma, PEL, and multicentric Castleman's disease [5]. Since KSHV-associated solid lymphoma possesses similar expression profiles of cellular and viral proteins to PEL, KSHV-associated solid lymphoma is thought to be an extra-cavity variant of PEL [8,9]. Although the molecular biological differences between PEL and KSHV-associated solid lymphoma remain unknown, PEL shows some unique characteristics in its clinical course compared with KSHV-associated solid lymphoma. For example, PEL